6586 *Inorg. Chem.* **2010**, *49*, 6586–6600
DOI: 10.1021/ic1004209

Inorganic Chemistry
Article

Polymer-Bound Oxidovanadium(IV) and Dioxidovanadium(V) Complexes As Catalysts for the Oxidative Desulfurization of Model Fuel Diesel

Mannar R. Maurya,*,† Aarti Arya,† Amit Kumar,‡ Maxim L. Kuznetsov,‡ Fernando Avecilla,§ and João Costa Pessoa*,‡

†*Department of Chemistry, Indian Institute of Technology Roorkee, Roorkee 247 667, India,* ‡*Centro Química Estrutural, Instituto Superior Técnico, TU Lisbon, Av Rovisco Pais, 1049-001 Lisboa, Portugal, and* §*Departamento de Química Fundamental, Universidade da Coruña, Campus de A Zapateira, 15071 A Coruña, Spain*

Received March 3, 2010

The Schiff base (Hfsal-dmen) derived from 3-formylsalicylic acid and *N,N*-dimethyl ethylenediamine has been covalently bonded to chloromethylated polystyrene to give the polymer-bound ligand, PS-Hfsal-dmen (**l**). Treatment of PS-Hfsal-dmen with $[V^{IV}O(acac)_2]$ in the presence of MeOH gave the oxidovanadium(IV) complex PS-$[V^{IV}O$(fsal-dmen)(MeO)] (**1**). On aerial oxidation in methanol, complex **1** was oxidized to PS-$[V^{V}O_2$(fsal-dmen)] (**2**). The corresponding neat complexes, $[V^{IV}O$(sal-dmen)(acac)] (**3**) and $[V^{V}O_2$(sal-dmen)] (**4**) were similarly prepared. All these complexes are characterized by various spectroscopic techniques (IR, electronic, NMR, and electron paramagnetic resonance (EPR)) and thermal as well as field-emission scanning electron micrographs (FE-SEM) studies, and the molecular structures of **3** and **4** were determined by single crystal X-ray diffraction. The EPR spectrum of the polymer supported $V^{IV}O$-complex **1** is characteristic of magnetically diluted $V^{IV}O$-complexes, the resolved EPR pattern indicating that the $V^{IV}O$-centers are well dispersed in the polymer matrix. A good ^{51}V NMR spectrum could also be measured with **4** suspended in dimethyl sulfoxide (DMSO), the chemical shift (−503 ppm) being compatible with a VO_2^+-center and a N,O binding set. The catalytic oxidative desulfurization of organosulfur compounds thiophene, dibenzothiophene, benzothiophene, and 2-methyl thiophene (model of fuel diesel) was carried out using complexes **1** and **2**. The sulfur in model organosulfur compounds oxidizes to the corresponding sulfone in the presence of H_2O_2. The systems **1** and **2** do not loose efficiency for sulfoxidation at least up to the third cycle of reaction, this indicating that they preserve their integrity under the conditions used. Plausible intermediates involved in these catalytic processes are established by UV−vis, EPR, ^{51}V NMR, and density functional theory (DFT) studies, and an outline of the mechanism is proposed. The ^{51}V NMR spectra recorded for solutions in methanol confirm that complex **4**, on treatment with H_2O_2, is able to generate peroxo-vanadium(V) complexes, including quite stable protonated peroxo-V^V-complexes $[V^{V}O(O)_2$(sal-dmen-$NH^+)]$. The ^{51}V NMR and DFT data indicate that formation of the intermediate hydroxido-peroxo-V^V-complex $[V^{V}(OH)(O_2)$(sal-dmen)$]^+$ does not occur, but instead protonated $[V^{V}O(O)_2$(sal-dmen-$NH^+)]$ complexes form and are relevant for catalytic action.

Introduction

The removal of sulfur from petroleum products has attracted much attention and has a strong economical impact in petrochemical industry. The sulfur present in the petroleum products is highly undesirable; it is responsible for poisoning of catalysts in petrochemical industries and, upon use of oil-derived products, it pollutes air, water, and soil, being harmful to health, and promotes acid rains. Researchers have developed several ways to remove sulfur from petroleum products. Hydrodesulfurization (HDS) is one of the common methods to produce ultra low sulfur fuels, but this process needs high temperature and pressure, thus requiring large consumption of energy and of hydrogen, which reduces the life of the catalysts used. The HDS process is highly efficient in removing thiols, sulfides, and disulfides, but less effective for thiophenes and thiophene derivatives. Thus, the sulfur compounds that remain in hydrodesulfurized fuels are mainly benzothiophene (BT), dibenzothiophene (DBT), and their alkylated derivatives.

Oxidative desulfurization (ODS) is another way to get ultra low sulfur fuels. In oxidative desulfurization processes, sulfur containing compounds are oxidized to sulfones. The sulfones are polar compounds and are easily separated from

*To whom correspondence should be addressed. E-mail: rkmanfcy@iitr.ernet.in (M.R.M.). Phone: +91 1332 285327 (M.R.M.). Fax: +91 1332 273560 (M.R.M.). E-mail: joao.pessoa@ist.utl.pt (J.C.P.). Phone: (+351) 21 841 92 68 (J.C.P.). Fax: (+351) 21 846 4455 (J.C.P.).

 Published on Web 06/21/2010

the fuel product by extraction, distillation, decomposition,[1] or adsorption on alumina.[2] For oxidative desulfurization, several oxidants like H_2O_2, *tert*-butylhydroperoxide (TBHP),[1,3] and organic acids have been reported,[4] but H_2O_2 is the most commonly used as it is cheap, non-polluting, and is an easily available commercial oxidant. The oxidation of organosulfur compounds such as sulfides, and dibenzothiophene (DBT) and their corresponding alkyl derivatives to sulfones[1c,3c,5,6] by H_2O_2 over various catalysts such as acetic acid,[6,7] formic acid,[8] polyoxometalate[9] and Ti-containing molecular sieves[1a,10] has been reported. The oxidation of organosulfur compounds has also been processed using various redox solid catalysts such as Ti-containing zeolites (TS-1, Ti-beta),[1a,11] titanium-hexagonal mesoporous silica,[12] V- or Mo-containing molecular sieves,[13] and solid bases such as hydrotalcites.[1c,5]

Oxidovanadium complexes have been used as catalysts for the oxidation of several organic compounds, epoxidation of alkenes and allyl alcohols, oxidative halogenations, and the oxidation of organic sulfides.[14] However, because of their homogeneous nature these catalysts are difficult to separate from the reaction mixture and, thus, cannot be recycled. Recently we have shown that grafting vanadium complexes on polymer support not only may improve their catalytic activities but also catalysts became recoverable and recyclable.[15] In the present work, we report polymer-bound oxidovanadium(IV) and dioxidovanadium(V) complexes of the polymer-bound ligand, PS-Hfsal-dmen (**I** Scheme 1) for the oxidation of thiophene derivatives present in diesel. No catalytic desulfurization using polymer-bound vanadium complexes as catalysts has been reported in the literature.[16] The anchoring to the polystyrene backbone provides extra stability to the catalysts and makes the catalytic reaction heterogeneous in nature. The neat complexes [$V^{IV}O$(sal-dmen)(acac)] (**3**) and [$V^{V}O_2$(sal-dmen)] (**4**) with the ligand, Hsal-dmen (**II**) having similar donor atoms has also been prepared for comparison of catalytic performance and recyclability.

Scheme 1. Structures of Ligands Used in This Work[a]

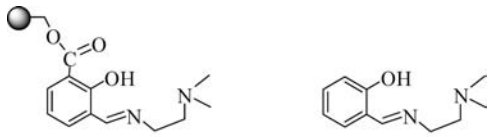

PS-Hfsal-dmen **I** Hsal-dmen **II**

[a] ●−− represents the polystyrene matrix.

Experimental Section

Materials. Chloromethylated polystyrene [18.9% Cl (5.35 mmol Cl per gram of resin)] cross-linked with 5% divinylbenzene was obtained as a gift from Thermax Limited, Pune, India. Analytical reagent grade V_2O_5 (Loba Chemie, Mumbai, India), *N*,*N*-dimethyl ethylenediamine, thiophene, dibenzothiophene, 2-methyl thiophene (Aldrich Chemicals Co., U.S.A), and salicylaldehyde (Ranbaxy, India) were used as obtained. Heptane (99.0%) was used as solvent of model compounds: thiophene, benzothiophene, dibenzothiophene, and 2-methyl thiophene. The model diesel fuel was prepared so that it contains 500 ppm S of thiophene, 500 ppm S of benzothiophene, 500 ppm S of dibenzothiophene, 500 ppm S of 2-methyl thiophene. An aqueous solution of hydrogen peroxide (30% H_2O_2) was used as the oxidizing agent. [$V^{IV}O(acac)_2$],[17] 3-formylsalicylic acid,[18] and ligands Hfsal-dmen[19] and Hsal-dmen[20] were prepared according to the methods reported.

Characterization Procedures. Elemental analyses of the ligands and complexes were obtained with an Elementar model

(1) (a) Hulea, V.; Fajula, F.; Bousquet, J. *J. Catal.* **2001**, *198*, 179–186. (b) Anisimov, A. V.; Fedorova, E. V.; Lesnugin, A. Z.; Senyavin, V. M.; Aslanov, L. A.; Rybakov, V. B.; Tarakanova, A. V. *Catal. Today* **2003**, *78*, 319–325. (c) Palomeque, J.; Clacens, J. M.; Figueras, F. *J. Catal.* **2002**, *211*, 103–108. (d) Yazu, K.; Yamamoto, Y.; Furuya, T.; Miki, K.; Ukegawa, K. *Energy Fuels* **2001**, *15*, 1535–1536. (e) Djangkung, S.; Murti, S.; Yang, H.; Choi, K.; Kora, Y.; Mochida, I. *Appl. Catal., A* **2003**, *252*, 331–346. (f) Shiraishi, Y.; Naito, T.; Hirai, T. *Ind. Eng. Chem. Res.* **2003**, *42*, 6034–6039.

(2) (a) Kazuhiko, S.; Koichi, A. *Oxidative Desulfurization of Fuel Oil.* Patent JP 2004196927, **2004**. (b) Yu, G. X.; Lu, S. X.; Chen, H.; Zhu, Z. *Energy Fuels* **2005**, *19*, 447–452. (c) Verduzco, L. F.; García, E. T.; Quintana, R. G. *Catal. Today* **2004**, *98*, 289–294. (d) Muratua, S.; Mirata, K.; Kidena, K.; Nomura, M. *Energy Fuels* **2004**, *18*, 116–121. (e) Zannikios, F.; Lois, E.; Stournas, S. *Fuel Process. Technol.* **1995**, *42*, 35–45.

(3) (a) Caero, L. C.; Forge, J.; Navarro, A.; Gutierrez-Alejandre, A. *Catal. Today* **2006**, *116*, 562–568. (b) Ramírez-Verduzco, L. F.; Torres-García, E.; Gomez-Quintana, R.; Gonzalez-Pena, V.; Murrieta-Guevara, F. *Catal. Today* **2004**, *98*, 289–294. (c) Figueras, F.; Palomeque, J.; Loridant, S.; Feche, C.; Essayem, N.; Gelbard, G. *J. Catal.* **2004**, *226*, 25–31.

(4) (a) Ramírez-Verduzco, L. F.; Murrieta-Guevara, F.; García-Gutierrez, J. L.; Saint Martin-Castanon, R.; Martinez-Guerrero, M.; Montiel-Pacheco, M.; Mata-Díaz, R. *Pet. Sci. Technol.* **2004**, *22*, 129–139. (b) Te, M.; Fairbridge, C.; Ring, Z. *Appl. Catal. A: Gen.* **2001**, *219*, 267–280.

(5) Dumitriu, E.; Guimon, C.; Cordoneanu, A.; Casenave, S.; Hulea, T.; Chelaru, C.; Martinez, H.; Hulea, V. *Catal. Today* **2001**, *66*, 529–534.

(6) Choudary, B. M.; Reddy, C. R. V.; Prakash, B. V.; Kantam, M. L.; Sreedhar, B. *Chem. Commun.* **2003**, 754–755.

(7) (a) Zannikos, F.; Lois, E.; Stournas, S. *Fuel Process. Technol.* **1995**, *42*, 35–45. (b) Bonde, S. E.; Gore, W.; Dolbear, G. E.; Skov, E. R. *Prepr.−Am. Chem. Soc., Div. Pet. Chem.* **2000**, *45*, 364–366. (c) Dolbear, G. E.; Skov, E. R. *Prepr.−Am. Chem. Soc., Div. Pet. Chem.* **2000**, *45*, 375–378. (d) Bonde, S. E.; Gore, W.; Dolbear, G. E. *Prepr.−Am. Chem. Soc., Div. Pet. Chem.* **1999**, *44*, 199–201. (e) Shiraishi, Y.; Tachibana, K.; Hirai, T.; Komasawa, I. *Ind. Eng. Chem. Res.* **2002**, *41*, 4362–4375.

(8) (a) Otsuki, S.; Nonaka, T.; Takashima, N.; Qian, W.; Ishihara, A.; Imai, T.; Kabe, T. *Energy Fuels* **2000**, *14*, 1232–1239. (b) Hill, C. L.; Prosser-McCartha, C. M. *Coord. Chem. Rev.* **1995**, *143*, 407–455.

(9) (a) Collins, F. M.; Andrew, R. L.; Christopher, S. *J. Mol. Catal. A* **1997**, *117*, 397–403. (b) Yatzu, K.; Yamamoto, Y.; Furuya, T.; Miki, K.; Ukegawa, K. *Energy Fuels* **2001**, *15*, 1535–1536.

(10) Shiraishi, Y.; Hirai, H.; Komosawa, I. *J. Chem. Eng. Jpn.* **2002**, *3*, 1305–1311.

(11) (a) Hulea, V.; Moreau, P.; Di Renzo, F. *J. Mol. Catal. A: Chem.* **1996**, *111*, 325–332. (b) Hulea, V.; Moreau, P. *J. Mol. Catal. A: Chem.* **1996**, *113*, 499–505. (c) Reddy, R. S.; Reddy, J. S.; Kumar, R.; Kumar, P. *J. Chem. Soc., Chem. Commun.* **1992**, 84–85.

(12) (a) Ziolek, M. *Catal. Today* **2004**, *90*, 145–150. (b) Trukhan, N. N.; Derevyankin, A.; Yu; Shmakov, A. N.; Paukshtis, E. A.; Kholdeeva, O. A.; Romannikov, V. N. *Microporous Mesoporous Mater.* **2001**, *44 −45*, 603–608.

(13) (a) Shiraishi, Y.; Naito, T.; Hirai, T. *Ind. Eng. Chem. Res.* **2003**, *42*, 6034–6039. (b) Raghavan, P. S.; Ramaswamy, V.; Upadhya, T. T.; Sudalai, A.; Ramaswamy, A. V.; Sivasanker, S. J. *J. Mol. Catal. A: Chem.* **1997**, *122*, 75–80.

(14) (a) Sheldon, R. A. *J. Mol. Catal.* **1980**, *7*, 107–126. (b) Sobczak, J.; Ziolkovski, J. J. *J. Mol. Catal.* **1981**, *13*, 11–42. (c) Sheldon, R. A.; Kochi, J. K. *Metal-catalyzed Oxidation of Organic Compounds*, Academic Press: New York, 1981. (d) Chang, C. J.; Labinger, J. A.; Gray, H. B. *Inorg. Chem.* **1997**, *36*, 5927–5930.

(15) (a) Maurya, M. R.; Kumar, U.; Manikandan, P. *Eur. J. Inorg. Chem.* **2007**, 2303–2314. (b) Maurya, M. R.; Kumar, U.; Correia, I.; Adão, P.; Costa Pessoa, J. *Eur. J. Inorg. Chem.* **2008**, 577–587. (c) Maurya, M. R.; Kumar, M.; Kumar, A.; Costa Pessoa, J. *Dalton Trans.* **2008**, 4220–4232. (d) Maurya, M. R.; Arya, A.; Kumar, A.; Costa Pessoa, J. *Dalton Trans.* **2009**, 2185–2195. (e) Maurya, M. R.; Arya, A.; Kumar, U.; Kumar, A.; Costa Pessoa, J. *Dalton Trans.* **2010**, *39*, 1345–1360.

(16) (a) Tkhai, F. V.; Tarakanova, A. V.; Kostyuchenko, O. V.; Tarasevich, B. N.; Kulikov, N. S.; Anisimov, A. V. *Theor. Found. Chem. Eng.* **2008**, *42*, 636–642. (b) Gómez-Bernal, H.; Cedeño-Caero, L.; Gutiérrez-Alejandre, A. *Catal. Today* **2009**, *142*, 227–233. (c) Cedeño-Caero, L.; Gomez-Bernal, H.; Fraustro-Cuevas, A.; Guerra-Gomez, H. D.; Cuevas-Garcia, R. *Catal. Today* **2008**, *133−135*, 244–254. (d) Xu, D.; Zhu, W.; Li, H.; Zhang, J.; Zou, F.; Shi, H.; Yan, Y. *Energy Fuels* **2009**, *23*, 5929–5933. (e) Cedeño-Caero, L.; Hernández, E.; Pedraza, F.; Murrieta, F. *Catal. Today* **2005**, *107−108*, 564–569.

(17) Rowe, R. A.; Jones, M. M. *Inorg. Synth.* **1957**, *5*, 113–116.

Vario-EL-III. Vanadium content in polymer-bound complexes was checked by Inductively Coupled Plasma spectrometry (ICP; Labtam 8440 plasma lab). The metal ion loadings calculated from the obtained vanadium content (1.65 mmol g^{-1} of resin for PS-[VO(fsal-dmen)(MeO)] **1**, and 1.43 mmol g^{-1} of resin for PS-[VO_2(fsal-dmen)] **4**) are also close to the values determined by thermogravimetric analysis (TGA). IR spectra were recorded as KBr pellets on a Nicolet NEXUS Aligent 1100 FT-IR spectrometer. Electronic spectra of the polymer-bound complexes were recorded in Nujol on a Shimadzu 1601 UV−vis spectrophotometer by layering a mull of the sample on the inside of one of the cuvettes while keeping the other one layered with Nujol as reference. Spectra of non-polymer bound ligand and complexes were recorded in methanol. ^{1}H NMR and ^{51}V NMR spectra were obtained on a Bruker Avance III 400 MHz spectrometer with the common parameter settings. NMR spectra were usually recorded in MeOD-d_4 or DMSO-d_6, and δ (^{51}V) values are referenced relative to neat $VOCl_3$ as external standard. Thermogravimetric analyses of the complexes were carried out using Perkin-Elmer (Pyris Diamond) under oxygen atmosphere. The energy dispersive X-ray analyses (EDX) of anchored ligand and complexes were recorded on a FEI Quanta 200 FEG. The samples were coated with a thin film of gold to prevent surface charging, to protect the surface material from thermal damage by the electron beam, and to make the sample conductive. Electron paramagnetic resonance (EPR) spectra were recorded with a Bruker ESP 300E X-band spectrometer. The spin Hamiltonian parameters were obtained by simulation of the spectra with the computer program of Rockenbauer and Korecz.[21] A Thermax Nicolet gas chromatograph fitted with a HP-1 capillary column (30 m × 0.25 mm × 0.25 μm) and FID detector was used to analyze the reaction products, and their quantifications were made on the basis of the relative peak area of the respective product. The identity of the products was confirmed using a GC-MS Perkin-Elmer, model Clarus 500 and comparing the fragments of each product with the library available.

Preparations. Preparation of PS-Hfsal-dmen (I). Chloromethylated polystyrene (3.0 g) was allowed to swell in *N*,*N*-dimethylformamide (DMF, 40 mL) for 2 h. A solution of Hfsal-dmen (10.63 g, 45 mmol) in DMF (30 mL) was added to the above suspension followed by triethylamine (4.50 g) in ethylacetate (40 mL). The reaction mixture was heated at 90 °C for 20 h with slow mechanical stirring in an oil bath. After cooling to room temperature, the red resins were separated by filtration, washed thoroughly with hot DMF followed by hot methanol, and dried in an air oven at 120 °C. Found: C, 74.0; H, 9.2; N, 7.0%.

Reaction of 3-fsal-dmen with Benzylchloride. A solution of 3-fsal-dmen (2.36 g, 10 mmol) in acetonitrile (40 mL) was added to the benzyl chloride (2.53 g, 20 mmol) solution followed by triethylamine (3.0 g) in ethylacetate (30 mL), and the reaction mixture was heated at about 80 °C for 36 h with continuous stirring. After evaporating the solvent and cooling to room temperature an orange product was obtained. Its purification by silica gel column chromatography and elution with MeOH/EtOAc (6:4) yielded a major waxy product. ^{1}H NMR (DMSO-d_6, δ/ppm): 10.4 (s, 1H, −OH), 8.15 (s, 1H, Ar−CH=N-), 6.67−8.37 (m, 8 H, aromatic), 5.30 (s, 2H, $-CH_2-$), 3.73, 3.40(t, 2H each, $-CH_2CH_2-$), 2.34 (s, 6H, $-CH_3$).

Preparation of PS-[V^{IV}O(fsal-dmen)(MeO)] (1). The polymer-bound ligand PS-fsal-dmen (1.50 g) was allowed to swell in DMF (25 mL) for 2 h. A solution of [$V^{IV}O(acac)_2$] (5.30 g, 20 mmol) in 20 mL of DMF was added to the above suspension, and the reaction mixture was heated at 90 °C in an oil bath for 15 h with slow mechanical stirring. After cooling to room temperature, the dark black polymer-bound complex obtained was separated by filtration, washed with hot DMF followed by hot methanol and dried at 120 °C in an air oven. Found: C, 71.9; H, 7.5; N, 5.2; V, 8.6%. This procedure was designed to prepare PS-[V^{IV}O(fsal-dmen)(acac)]. However, EPR measurements indicate that the acetylacetonato ligand is not coordinated to the $V^{IV}O$ center, and we suggest PS-[V^{IV}O(fsal-dmen)(MeO)] as a plausible formulation for this polymer-bound complex. Upon contact of **1** with dimethyl sulfoxide (DMSO) for 15 h, the presence of MeO^- was confirmed by the detection (by GC-MS) of MeOH in the liquid part of this mixture (see Supporting Information).

Preparation of PS-[$V^{V}O_2$(fsal-dmen)] (2). Complex **1** (1.5 g) was suspended in 50 mL MeOH and air was bubbled for about 48 h. During this period the color of the beads slowly changed to orange; these were filtered off, washed with MeOH and dried at room temperature over silica gel. Found: C, 65.2; H, 7.3; N, 7.5; V, 13.0%. A good ^{51}V NMR signal was measured with **2** suspended in DMSO, consisting of a reasonably strong resonance at δ = −503 ppm (broad, line width at half height of ca. 300 Hz).

[V^{IV}O(sal-dmen)(acac)] (3). A stirred solution of Hsal-dmen (0.96 g, 5 mmol) in methanol (10 mL) was treated with [$V^{IV}O(acac)_2$] (1.33 g, 5 mmol) dissolved in methanol (20 mL), and after an initial stirring for 1 h the resulting reaction mixture was refluxed for 1 h. The brown, X-ray-quality crystals formed upon slow evaporation were collected and dried under vacuum. Yield 85%. Anal. Calcd. For $C_{16}H_{22}N_2O_4V$: C, 53.8; H, 6.2; N, 7.8; V, 14.3%. found: C, 54.3; H, 6.4; N, 7.8; V, 14.2%.

[$V^{V}O_2$(sal-dmen)] (4). Complex **3** (0.27 g, 1 mmol) was dissolved in methanol. Air was bubbled through the solution slowly giving a yellow solution within 24 h. The crystals of **4** with suitable quality for single-crystal X-ray diffraction formed on slow evaporation of the solution were filtered and dried in air. Yield 70%. Anal. Calcd. For $C_{11}H_{15}N_2O_3V$: C, 48.2; H, 5.5; N, 10.2; V, 18.6%. Found: C, 48.2; H, 5.3; N, 10.2; V, 18.6%. ^{1}H NMR (MeOD-d_4, δ/ppm): 6.8−7.5 (m, 4 H, aromatic), 8.9 (s, 1H, Ar−CH=N), 4.22, 3.62(t, 2H each, $-CH_2CH_2-$), 2.88 (s, 6H). ^{51}V NMR (MeOD-d_4, δ/ppm): −502 (ca. 2.4%), −515 (ca. 5.6%) and −544 (ca. 92%). ^{51}V NMR (DMSO-d_6, δ/ppm): −503 (ca. 92%) and −490 (ca. 8%).

X-ray Crystal Structure Determination. Three-dimensional X-ray data for **3** and **4** were collected on a Bruker Kappa X8 Apex CCD diffractometer by the $\phi-\omega$ scan method. Data was collected at low temperature. Reflections were measured from a hemisphere of data collected of frames each covering 0.3 degrees in ω. Of the 11502 in **3** and 75059 in **4** reflections measured, all of which were corrected for Lorentz and polarization effects, and for absorption by semiempirical methods based on symmetry-equivalent and repeated reflections, 1716 in **3** and 24423 in **4** independent reflections exceeded the significance level $|F|/\sigma(|F|) > 4.0$. Complex scattering factors were taken from the program package SHELXTL.[22] The structures were solved by direct methods and refined by full-matrix least-squares methods on F^2. The non-hydrogen atoms were refined with anisotropic thermal parameters in all cases. In **3** the hydrogen atoms were left to refine freely in all cases, except for C9, and were included in calculated positions and refined by using a riding mode for all the atoms of **3**. For **3**, the absolute configuration was established by refinement of the enantiomorph polarity parameter [x = 0.557(13)].[23] The space group is $P1$; however, there is pseudo-symmetry[24] which emulates a centered unit cell in $Pca2_1$, but it is not supported by the diffraction pattern, which is consistent

(18) Duff, J. C.; Bills, E. J. *J. Chem. Soc.* **1923**, 1987.
(19) Floriana, T.; Luminita, P.; Marius, A. *Synth. React. Inorg., Met.-Org. Chem.* **1998**, *28*, 13–22.
(20) Karmakar, R.; Choudhury, C. R.; Hughes, D. L.; Yap, G. P.A.; Fallah, M. S.; El; Desplanches, C.; Sutter, J.-P.; Mitra, S. *Inorg. Chim. Acta* **2006**, *359*, 1184–1192.
(21) Rockenbauer, A.; Korecz, L. *Appl. Magn. Reson.* **1996**, *10*, 29–43.
(22) Sheldrick, G. M. *SHELXL-97: An Integrated System for Solving and Refining Crystal Structures from Diffraction Data*, Revision 5.1; University of Göttingen: Göttingen, Germany, 1997.
(23) Bernardinelli, G.; Flack, H. D. *Acta Crystallogr., Sect. A* **1985**, *41*, 500–511.

with the correct space group *P*1. A final difference Fourier map showed no residual density outside: 0.602, −0.591 e Å^{-3} in **4** and 0.613, −0.584 e Å^{-3} in **3**. The crystal data and details on data collection and refinement are summarized in Supporting Information, Table S1. CCDC-766123 (for **3**) contains the supplementary crystallographic data for this paper. This data can be obtained free of charge from the Cambridge Crystallographic Data Centre via www.ccdc.cam.ac.uk/data_request/cif.

DFT Computational Details. The full geometry optimization of all structures envisaged has been carried out at the DFT level of theory using B3LYP,[25a,b] B3P86,[25a,c] and, for some structures, B3PW91[25a,d] functionals with the help of the Gaussian-03[26] program package. No symmetry operations have been applied for any of the structures calculated. The geometry optimization was carried out using a relativistic Stuttgart pseudopotential that described 10 core electrons and the appropriate contracted basis set (8s7p6d1f)/[6s5p3d1f][27] for the vanadium atom and the 6-31G-(d) basis set for other atoms. The Hessian matrix was calculated analytically for all optimized structures to prove the location of correct minima (no imaginary frequencies) and to estimate the thermodynamic parameters, the latter being calculated at 25 °C. The comparison of the calculated structural parameters and ^{51}V chemical shifts of **CI** with experimental values indicated that the B3P86 functional usually reproduces both types of properties better than B3LYP or B3PW91 functionals (see Supporting Information for details). Hence, only results obtained using the B3P86 functional are discussed further.

Total energies corrected for solvent effects (E_s) were estimated at the single-point calculations on the basis of gas-phase geometries at the CPCM-B3P86/6-311+G(2d,p)//gas-B3P86/6-31G(d) level of theory using the polarizable continuum model[28] in the CPCM version[29] with methanol and heptane as solvents. The UAKS model was applied for the molecular cavity. The entropic term in solutions (S_s) was calculated according to the procedure described by Wertz,[30] and Cooper and Ziegler[31] (see Supporting Information for details). The enthalpies and Gibbs free energies in solution (H_s and G_s) were estimated using the following equations

$$H_s = E_s(\text{6-311+G(2d,p)}) + H_g(\text{6-31G(d)}) - E_g(\text{6-31G(d)})$$

$$G_s = H_s - TS_s$$

where E_s, E_g, and H_g are the total energies in solution and in gas phase and gas-phase enthalpy calculated at the corresponding level.

Magnetic shieldings were calculated for the equilibrium geometries using the GIAO[32] method at the CPCM-B3P86/6-311+G(2d,p)//gas-B3P86/6-31G(d) level including the solvent effects with methanol as solvent. The ^{51}V chemical shifts were estimated relative to $VOCl_3$ (σ of −2914 calculated at the same level of theory). It is known[33] that calculated ^{51}V chemical shifts of peroxo-complexes relative to $VOCl_3$ differ significantly from the experimental values, and the difference is much higher than that in the case of oxido-complexes. Such a systematic error is explained by different shielding properties of the V atom in complexes bearing only oxido-ligands (as in the $VOCl_3$ standard) and in the species having peroxo-ligands. However, the usage of a second reference compound (a V-complex with peroxo-ligand) allows the introduction of an empirical correction and the reduction of this error. Hence, for the theoretical estimates of δ_V in peroxo-complexes, another reference compound bearing the peroxo-ligand is required, but we could not find in the literature this type of correction to be used for V-peroxo complexes. In this article, complex $[V(=O)(OO)(ox)(bpy)]^-$ (ox = oxalate, bpy = 2,2′-bipyridine) was used as the second reference compound, and the choice was caused by the fact that it bears both oxido and peroxo ligands and does not change the composition in water solution for a long time.[34] The empirical correction of −42 ppm was introduced for the peroxo-complexes **CIII**, **CIV**, **CVIII**, and **CIX**, and it was calculated as follows: the ^{51}V chemical shift relative to $VOCl_3$ in water solution was calculated for the second reference compound, ($[V(=O)(OO)(ox)(bpy)]^-$, σ_{calc} = −2341, δ_{Vcalc} = −573 ppm). The comparison with the experimental value (−615.4 ppm[34]) gives the difference 42 ppm. Such an approach was used recently by Sarotti and Pellegrinet[35] for the calculations of ^{13}C chemical shifts. It is important that in the case of thus corrected chemical shifts, $VOCl_3$ is still used as the fundamental reference standard, and, hence, they may be compared with experimental δ_V values.

Catalytic Reaction. Oxidation of Organosulfur Compounds. The oxidation of the model diesel organosulfur compounds was carried out in 50 mL two-neck reaction flasks fitted with a water condenser. The polymer-bound complex was allowed to swell in heptane for 2 h prior to use in each experiment. The solution of the different organosulfur compounds [thiophene (T), 2-methylthiophene (2-MT), dibenzothiophene (DBT), and benzothiophene (BT)] with sulfur concentrations of 500 ppm was dissolved in 100 mL of heptane. In a typical reaction, 10 mL of 500 ppm sulfur containing organosulfur compounds (i.e., 2.25 mmol of T, 0.884 mmol of BT, 0.468 mmol of DBT, 1.725 mmol of MT), 30% H_2O_2 (3 times of the corresponding organosulfur compound, i.e., oxidant/substrate ratio of 3: 1) and catalyst, PS-[V^VO_2(fsal-dmen)] (0.0715 mmol) were taken in a reaction flask and stirred at 60 °C for 2 h. The progress of the reaction was monitored every 10 min by withdrawing small amounts of the reaction mixture and analyzing the samples quantitatively by gas chromatography. The identity of the products was confirmed by GC-MS. The effect of various parameters such as temperature, amount of oxidant and catalyst were studied to obtain the reaction conditions for the best performance of the catalyst.

Results and Discussion

Synthesis and Characterization of Catalysts. The Hfsaldmen ligand, obtained by the condensation of 3-formylsalicylic acid and *N*,*N*-dimethylethylenediamine, reacted

(24) Guzei, I. A.; Roberts, J.; Saulys, D. A. *Acta. Crystallogr., Sect. C* **2002**, *58*, m14–m143.
(25) (a) Becke, A. D. *J. Chem. Phys.* **1993**, *98*, 5648–5652. (b) Lee, C.; Yang, W.; Parr, R. G. *Phys. Rev.* **1988**, *B37*, 785–789. (c) Perdew, J. P. *Phys. Rev. B* **1986**, *33*, 8822–8824. (d) Perdew, J. P.; Burke, K.; Wang, Y. *Phys. Rev. B* **1996**, *54*, 16533–16539.
(26) Frisch, M. J.; Trucks, G. W.; Schlegel, H. B.; Scuseria, G. E.; Robb, M. A.; Cheeseman, J. R.; Montgomery, J. A.; Vreven, Jr., T.; Kudin, K. N.; Burant, J. C.; Millam, J. M.; Iyengar, S. S.; Tomasi, J.; Barone, V.; Mennucci, B.; Cossi, M.; Scalmani, G.; Rega, N.; Petersson, G. A.; Nakatsuji, H.; Hada, M.; Ehara, M.; Toyota, K.; Fukuda, R.; Hasegawa, J.; Ishida, M.; Nakajima, T.; Honda, Y.; Kitao, O.; Nakai, H.; Klene, M.; Li, X.; Knox, J. E.; Hratchian, H. P.; Cross, J. B.; Bakken, V.; Adamo, C.; Jaramillo, J.; Gomperts, R.; Stratmann, R. E.; Yazyev, O.; Austin, A. J.; Cammi, R.; Pomelli, C.; Ochterski, J. W.; Ayala, P. Y.; Morokuma, K.; Voth, G. A.; Salvador, P.; Dannenberg, J. J.; Zakrzewski, V. G.; Dapprich, S.; Daniels, A. D.; Strain, M. C.; Farkas, O.; Malick, D. K.; Rabuck, A. D.; Raghavachari, K.; Foresman, J. B.; Ortiz, J. V.; Cui, Q.; Baboul, A. G.; Clifford, S.; Cioslowski, J.; Stefanov, B. B.; Liu, G.; Liashenko, A.; Piskorz, P.; Komaromi, I.; Martin, R. L.; Fox, D. J.; Keith, T.; Al-Laham, M. A.; Peng, C. Y.; Nanayakkara, A.; Challacombe, M.; Gill, P. M. W.; Johnson, B.; Chen, W.; Wong, M. W.; Gonzalez, C.; Pople, J. A. *Gaussian 03*, revision D.01; Gaussian, Inc.: Wallingford, CT, 2004.
(27) Dolg, M.; Wedig, U.; Stoll, H.; Preuss, H. *J. Chem. Phys.* **1987**, *86*, 866–872.
(28) Tomasi, J.; Persico, M. *Chem. Rev.* **1994**, *94*, 2027–2094.
(29) Barone, V.; Cossi, M. *J. Phys. Chem. A* **1998**, *102*, 1995–2001.
(30) Wertz, D. H. *J. Am. Chem. Soc.* **1980**, *102*, 5316–5322.
(31) Cooper, J.; Ziegler, T. *Inorg. Chem.* **2002**, *41*, 6614–6622.
(32) (a) Ditchfield, R. *Mol. Phys.* **1974**, *27*, 789. (b) Wolinski, K.; Hinton, J. F.; Pulay, P. *J. Am. Chem. Soc.* **1990**, *112*, 8251–8260.
(33) Justino, L. L. G.; Ramos, M. L.; Nogueira, F.; Sobral, A. J. F. N.; Geraldes, C. F. G. C.; Kaupp, M.; Burrows, H. D.; Fiolhais, C.; Gil, V. M. S. *Inorg. Chem.* **2008**, *47*, 7317–7326.
(34) Tatiersky, J.; Schwendt, P.; Marek, J.; Sivák, M. *New. J. Chem.* **2004**, *28*, 127–133.
(35) Sarotti, A. M.; Pellegrinet, S. C. *J. Org. Chem.* **2009**, *74*, 7254–7260.

Scheme 2. - Synthesis of the PS-Anchored Ligand **I**

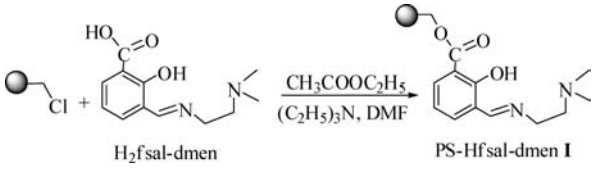

Scheme 3. Reaction of PS-Hfsal-dmen **I** with $[V^{IV}O(acac)_2]$ in DMF/MeOH[a]

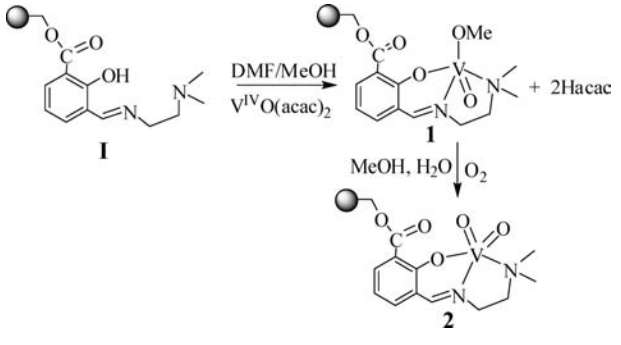

[a] The procedure was designed to prepare PS-[V^{IV}O(fsal-dmen)(acac)], but as evaluated by EPR, the polymer-anchored V^{IV}O-complex obtained does not contain a bidentate coordinated acetylacetonato ligand. The presence of the MeO^- ligand was confirmed by GC-MS (see Supporting Information).

with chloromethylated polystyrene to give the polystyrene supported ligand, PS-Hfsal-dmen **I**. In this process, the −COOH group of 3-formylsalicylic acid reacted with the $-CH_2Cl$ group of polystyrene as shown in Scheme 2. Reaction of the −COOH group of 3-formylsalicylic acid with $-CH_2Cl$ was further demonstrated by the reaction of benzyl chloride with Hfsal-dmen in CH_3CN in presence of triethylamine. The remaining chlorine content of 1.5% (0.51 mmol Cl g^{-1} of resin) in PS-Hfsal-dmen suggests about 90% loading of the ligand.

The polymer-bound ligand **I** on reaction with $[V^{IV}O(acac)_2]$ in DMF at about 90 °C affords the polymer-bound complex, PS-[V^{IV}O(fsal-dmen)(MeO)] **1**. Complex **1** on aerial oxidation in MeOH, yields the dioxidovanadium(V) complex, PS-$[V^{V}O_2$(fsal-dmen)] **2**. The synthetic procedures are outlined in Scheme 3. Similarly, the reaction of $[V^{IV}O(acac)_2]$ with an equimolar amount of Hsal-dmen in refluxing methanol gave the oxidovanadium(IV) complex, [V^{IV}O-(sal-dmen)(acac)] **3** which on aerial oxidation gave the dioxidovanadium(V) complex, $[V^{V}O_2$(sal-dmen)] **4**.

Table 1 provides data of metal and ligand loading in polymer-bound complexes, assuming the formation of PS-Hfsal-dmen. The obtained data show that the metal to ligand ratio in polymer-bound complexes is close to 1:1.

Description of Structure of [VO(acac)(sal-dmen)] (3). In the study of heterochelates of coordination type [V^{V}OLL′] based on tridentate L (ONO[36,37] or ONN,[38,39]) and bidentate L′ (ON[37] Schiff base ligands or in some OO[36,37])

Table 1. Ligand and Metal Loadings in Polymer-Bound Complexes, and Ligand-to-Metal Ratio Data

compound	ligand loading (mmol g^{-1} of resin)	metal ion loading[a] (mmol g^{-1} of resin)	ligand/metal ratio
PS-[Hfsal-dmen] **I**	2.4		
PS-[V^{IV}O(fsal-dmen)(MeO)]	1.8	1.65	1: 1.09
PS-$[V^{V}O_2$(fsal-dmen)]	1.6	1.43	1: 1.12

[a] Metal ion loading = (observed metal % × 10)/(atomic weight of metal); the values for the metal ion loading are based on the vanadium content determined by ICP.

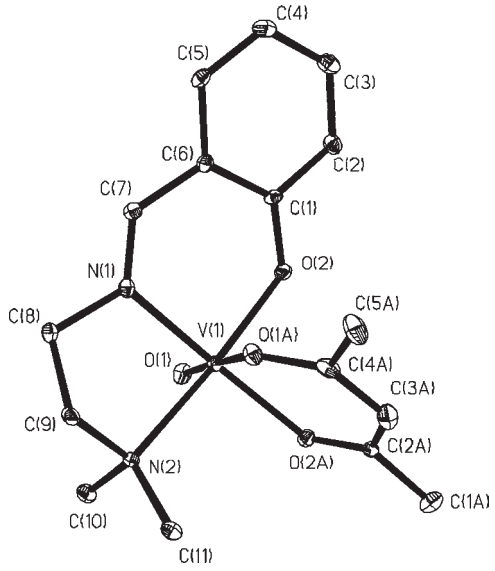

Figure 1. ORTEP diagram of [V^{IV}O(sal-dmen)(acac)] **3**. All the non-hydrogen atoms are represented by their 30% probability ellipsoids. Hydrogen atoms are omitted for clarity.

donating ligands, the tridentate ligand L normally occupies three positions in the equatorial plane, and the fourth position is occupied for an O or N atom of the bidentate ligand L′. This is partially due to the planar nature of neat tridentate ligands included in the studies.

In complex **3**, the structure consists of eight independent vanadium monomers per asymmetric unit (Figure 1). In each monomer, the VO_4N_2 coordination sphere is a distorted octahedron with one of the O-acac donor atoms bound *trans* to the O-oxido atom. The calculated Flack parameter indicates the presence of racemic twinning. The VO_4N_2 coordination sphere is a distorted octahedron in which the vanadium atoms are displaced from the plane of the four equatorial donor atoms toward the O-oxido atom by an average of 0.286 Å (in the range: 0.2757−0.2968 Å). Table 2 includes selected bond lengths and angles for **3**, and the Supporting Information includes more details. The V=O distances are in the range 1.604(3)−1.613(3) Å (average: 1.608 Å) and are slightly longer than the range defined for other neutral V^{IV}O-complexes of 1.55−1.60 Å.[40] The V−O_{phe} lengths are in

(36) Barua, B.; Das, S.; Chakravorty, A. *Inorg. Chem.* **2002**, *41*, 4502–4508.
(37) Rath, S. P.; Ghosh, T.; Mondal, S. *Polyhedron* **1997**, *16*, 4179–4186.
(38) Cornman, C. R.; Colpas, G. J.; Hoeschele, J. D.; Kampf, J.; Pecoraro, V. L. *J. Am. Chem. Soc.* **1992**, *114*, 9925–9933.
(39) Cornman, C. R.; Kampf, J.; Lah, M. S.; Pecoraro, V. L. *Inorg. Chem.* **1992**, *31*, 2035–2043.
(40) (a) Vilas Boas, L. F.; Costa Pessoa, J. *Comprehensive Coordination Chemistry*; Wilkinson, G., Gillard, R.D., McCleverty, J.A., Eds.; Pergamon Press: Oxford, 1987; Vol *3*, Chapter 33, pp 453−583. (b) Crans, D. C.; Smee, J. J., *Comprehensive Coordination Chemistry II*; McCleverty, J.A., Meyer, T.J., Eds.; Elsevier: Amsterdam, 2004; Vol. *4*, pp 175−239.

Table 2. Selected Bond Lengths and Angles for Compounds **3** and **4**[a]

4	Å	**4**	(deg)	**4**	(deg)
V(1)−O(2)	1.604(2)	O(2)−V(1)−O(3)	109.75(12)	O(3)−V(1)−N(2)	88.66(11)
V(1)−O(3)	1.621(2)	O(2)−V(1)−O(1)	105.13(10)	O(1)−V(1)−N(2)	154.24(9)
V(1)−O(1)	1.911(2)	O(3)−V(1)−O(1)	98.28(11)	N(1)−V(1)−N(2)	75.60(9)
V(1)−N(1)	2.147(2)	O(2)−V(1)−N(1)	107.13(11)		
V(1)−N(2)	2.185(2)	O(3)−V(1)−N(1)	141.05(11)		
N(1)−C(7)	1.280(4)	O(1)−V(1)−N(1)	83.71(9)		
N(1)−C(8)	1.460(4)	O(2)−V(1)−N(2)	95.63(11)		
O(1)−C(1)	1.331(3)	O(2)−V(1)−N(2)	95.63(11)		
3	Å	**3**	(deg)	**3**	(deg)
V(1)−O(1)	1.604(3)	O(1)−V(1)−O(2)	100.67(13)	N(1)−V(1)−O(1A)	78.01(12)
V(1)−O(2)	1.956(3)	O(1)−V(1)−O(2A)	99.57(13)	O(1)−V(1)−N(2)	91.58(13)
V(1)−O(2A)	1.991(3)	O(2)−V(1)−O(2A)	92.06(12)	O(2)−V(1)−N(2)	165.75(12)
V(1)−N(1)	2.063(3)	O(1)−V(1)−N(1)	98.87(14)	O(2A)−V(1)−N(2)	93.04(12)
V(1)−O(1A)	2.187(3)	O(2)−V(1)−N(1)	89.08(12)	N(1)−V(1)−N(2)	81.82(12)
V(1)−N(2)	2.223(3)	O(2A)−V(1)−N(1)	160.98(12)	O(1A)−V(1)−N(2)	82.66(11)
N(1)−C(7)	1.278(5)	O(1)−V(1)−O(1A)	173.77(12)		
N(1)−C(8)	1.471(5)	O(2)−V(1)−O(1A)	84.75(11)		
C(1)−O(2)	1.306(5)	O(2A)−V(1)−O(1A)	83.18(11)		

[a] Bond lengths and angles are given only for one of the eight independent vanadium monomers of compound **3**.

the range 1.955(3)−1.960(3) Å (average: 1.957 Å) and are longer than in other similar compounds such as [VO(salhyb)(Q)], [VO(salhyp)(Q)], and [VO(salhyh)(Q)],[41] which are in the range of 1.85−1.87 Å, but are similar to those of compounds with a N-atom in *trans* position in respect to the phenolate-O atom.[42] The vanadium-imine-N atom distances are in the range 2.057(3)−2.063(3) Å (average: 2.060 Å, see Table 2 and S2) and are similar to other V−N-imine bond lengths reported for other similar compounds, for example, [VO(cat)(gsal)],[36] [VO(tBu_2-cat)(vsal)],[36] [VO(hshed)(shi)],[38] [VO(cat)(salimh)],[38] [VO(sal)(salimh)],[39] [VO(acac)(salimh)],[39] [VO(acac)(hshed)],[43a] [VO(acac)(sal-aebmz)],[43b] [VO(bha)(sal-aebmz)],[43b] and [VO(acac)(salimRH)].[42]

As is common in oxidovanadium compounds, the weakest bond is to the donor atom *trans* to the oxido-O atom. The longer bond of the $acac^-$ ligand is *trans* to the oxido-O atom, close to 2.2 Å (see Table 2). Although the carbon−carbon and carbon−oxygen distances of the $acac^-$ ligand do not allow to differentiate the ketonic oxygen from the enolic oxygen one, the similarity of the structure of **3** with that of [VO(acac)(salimh)][39] suggests that the neutral carbonyl-O atom is in the axial position.

Description of Structure of [VO_2(sal-dmen)] (4). The structure of this compound was previously reported[44] (see Supporting Information), and the distances and angles obtained for **4** are very close to the structure previously published. The unit cell contains discrete monomeric molecules. The vanadium(V) ion is five-coordinate, with a distorted square pyramidal environment. The metal ion lies 0.4782 Å above the mean plane of atoms O1, O3, N1, N2 in the direction of the axial oxido ligand, O2. The τ value for this geometry is 0.22 indicating a significant distortion toward the trigonal bipyramidal form. Table 2 also includes selected bond lengths and angles of **4**, to be compared with those of **3**.

Field Emission-Scanning Electron Microscope (FE-SEM) and Energy Dispersive X-ray Analysis (EDX) studies. The change in morphology of polymer beads after the loading of ligand and metal ion was studied by FE-SEM micrographs and EDX analyses, and some of images of beads and of EDX are reproduced in Supporting Information, Figure S2. A considerable amount of N (ca. 8.7%) and a small amount of Cl (ca. 1.8%) were determined on the surface of the beads containing the anchored ligand. The polymer-bound ligand, PS-Hfsal-dmen shows the smooth and flat surface (Supporting Information, Figure S2a) and after metal incorporation shows a very slight roughening of the top layer on the surface, because of the polymer-bound metal complexes (Supporting Information, Figures S2b and S2c). The presence of a very low content of chlorine and relatively good content of nitrogen on the surface of the grafted complexes suggests the replacement of chlorine by the carboxylic group. The presence of vanadium on the surface was semiquantitatively estimated to be 1.6% and 1.2% in PS-[$V^{IV}O$(fsal-dmen)(MeO)] and PS-[$V^{V}O_2$(fsal-dmen)], respectively. Accurate information on the morphological changes in terms of exact orientation of ligand coordinated to the metal ion has not been possible because of low amount of the metal complex on polymer surface.

TGA Studies. The polymer-bound complexes PS−[$V^{IV}O$(fsal-dmen)(MeO)] and PS−[$V^{V}O_2$(fsal-dmen)] are thermally stable up to about 175 °C. Both complexes, thereafter, decompose in two steps. Quantitative measurement of weight loss at various stages was not possible because of their overlapping nature. However, the stability of final residues at about 700 °C suggests the formation of V_2O_5. The amount of final product was used to estimate the percentage of vanadium in the polymer-bound complexes (1.7 mmol g^{-1} for **1** and 1.4 mmol g^{-1} for **2**). The values obtained by TGA therefore agree well with those obtained by ICP (1.65 mmol g^{-1} for **1** and 1.43 mmol g^{-1} for **2**).

(41) Nica, S.; Rudolph, M.; Görls, H.; Plass, W. *Inorg. Chim. Acta* **2007**, *360*, 1743–1752.
(42) Smith, T. S., II; Root, C. A.; Kampf, J. W.; Rasmussen, P. G.; Pecoraro, V. L. *J. Am. Chem. Soc.* **2000**, *122*, 767–775.
(43) (a) Li, X.; Lah, M. S.; Pecoraro, V. L. *Inorg. Chem.* **1988**, *27*, 4657–4664. (b) Maurya, M. R.; Kumar, A.; Ebel, M.; Rehder, D. *Inorg. Chem.* **2006**, *45*, 5924–5937.
(44) Xie, M.-J.; Ping, Y.; Zheng, L.-D.; Hui, J.-Z.; Peng, C. *Acta Crystallogr., Sect. E* **2004**, *60*, m1382–m1383.

Table 3. IR Spectral Data of Ligand and Complexes

compound	ν(C=O)	ν(C=N)	ν(V=O)
PS-Hfsal-dmen **I**	1669	1630	
PS-[$V^{IV}O$(fsal-dmen)(MeO)] **1**	1667	1601	974
PS-[$V^{V}O_2$(fsal-dmen)] **2**	1667	1629	923, 857
[$V^{IV}O$(sal-dmen)(acac)] **3**		1639	953
[$V^{V}O_2$(sal-dmen)] **4**		1630	925, 896
[$V^{V}O(O_2)$(sal-dmen)][a] **5**		1621[a]	957[a]

[a] Complex **5** is unstable and looses oxygen at room temperature; it could not be properly characterized (see text and Supporting Information)).

IR Spectral Study. The important IR bands for the neat and polymer-bound ligands and their vanadium complexes are given in Table 3. The chloromethylated polystyrene shows strong peaks at 1264 and 673 cm^{-1},[45] and absence of these peaks in PS-Hfsal-dmen suggests the covalent bonding of polystyrene with Hfsal-dmen. The polymer-bound ligand exhibits a sharp band at 1669 cm^{-1}due to the ν(C=O) of the carboxylic group. Existence of this band suggests covalent bond formation between the ligand and the polymer through a carboxylic acid group. In addition, PS-[$V^{IV}O$(fsal-dmen)(MeO)] exhibits a medium intensity band at 974 cm^{-1} due to ν(V=O); similarly complex PS-[$V^{V}O_2$(fsal-dmen)] **2** exhibits two such bands at 923 and 857 cm^{-1} corresponding to $\nu_{antisym}$ (O=V=O) and ν_{sym} (O=V=O) modes, respectively.[46] Neat vanadium complexes also exhibit spectral patterns compatible with those of the corresponding polymer-bound complexes, and also similar to those reported in literature.[47]

We prepared complex [$V^{V}O(O_2)$(sal-dmen)]; however, as it is unstable and looses oxygen at room temperature it could not be properly characterized. The freshly prepared complex gives an IR spectrum (Supporting Information, Figure S10) including peaks: (V=O, s) 957, (O−O, s) 886, (V−O_2, s, as) 610 cm^{-1} (see Supporting Information). These peaks agree well with those reported for several [$VO(O_2)$L] complexes,[48] being consistent with its formulation as a peroxo complex.

Electronic Spectral Data. The electronic spectra of polymer anchored and neat complexes are reproduced in Figures 2A and 2B, respectively, and the data are summarized in Table 4. Globally the electronic spectral patterns exhibited by the polymer-bound metal complexes are similar to those obtained for the corresponding non-polymer bound analogues, except the low intensity of some bands (Table 4). The spectrum of Hsal-dmen exhibits four bands at 401, 317, 255, and 216 nm. The bands at 255 and 216 nm are assignable to $\pi\rightarrow\pi^*$ transitions (B- and K-bands, respectively)[49] of the aromatic rings, while the first two bands may be associated to $n-\pi^*$ transitions. The bands at about 380 and 385 nm in oxidovanadium and dioxido-vanadium complexes, respectively, may be due to ligand to metal charge transfer (lmct) bands but may also contain bands localized in the

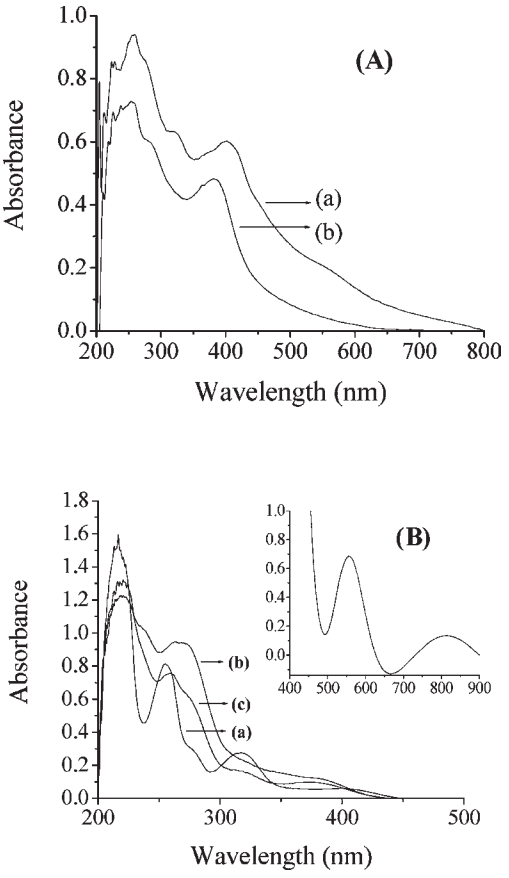

Figure 2. (A) Electronic spectra of (a) PS-[$V^{IV}O$(fsal-dmen)(MeO)] and (b) PS-[$V^{V}O_2$(fsal-dmen)] recorded with the compounds dispersed in nujol. (B) Electronic spectra of (a) Hsal-dmen, (b) [$V^{IV}O$(sal-dmen)(acac)] **3**, and (c) [$V^{V}O_2$(sal-dmen)] **4** recorded in MeOH (ca. 10^{-4} M). The inset shows the electronic spectrum of an about 10^{-3} M solution of **3**.

Table 4. Electronic Spectral Data of Ligand and Complexes[a]

compound	solvent	λ_{max} (nm)
PS-[$V^{IV}O$(fsal-dmen)(MeO)] **1**	Nujol	395, 316, 257
PS-[$V^{V}O_2$(fsal-dmen)] **2**	Nujol	389, 295, 254
Hsal-dmen **I**	MeOH	401, 317, 255, 216
[$V^{IV}O$(sal-dmen)(acac)] **3**	MeOH	813, 558, 380, 262, 221
[$V^{V}O_2$(sal-dmen)] **4**	MeOH	385, 319, 259, 220

[a] Freshly prepared [$VO(O_2)$(sal-dmen)] **5** gave a broad band at about 390 nm. This band probably includes transitions involving the C=N group as well as peroxo-to-vanadium charge transfer transitions.

C=N group. The bands at 813 and 558 nm in neat [$V^{IV}O$(sal-dmen)(acac)] are assigned to d−d transitions; they are not detected in the polymer-bound complex because of its poor loading in the polymer matrix.

^{51}V NMR Studies. In the present study we have reinvestigated complex **4** in solution, trying to establish speciation using ^{51}V NMR spectroscopy. The ^{51}V NMR spectrum of [$V^{V}O_2$(sal-dmen)] **4** (ca. 4 mM) dissolved in DMSO-d_6 shows a strong resonance at $\delta = -503$ ppm (92.0%) and a minor resonance at −490 ppm (8.0%). For the same complex dissolved in MeOH resonances at $\delta = -515$ (92.0%), together with two minor signals at about −502 ppm (2.4%) and −544 ppm (5.6%), were recorded (Figure 3a). The assignment of these and other resonances was done by considering both the experiments described below and DFT calculations. Addition of methanol (50% v/v) to a

(45) Arroyo, P.; Gil, S.; Munoz, A.; Palanca, P.; Sanchis, J.; Sanz, V. *J. Mol. Catal. A: Chem.* **2000**, *160*, 403–408.
(46) Maurya, M. R. *Coord. Chem. Rev.* **2003**, *237*, 163–181.
(47) Syamal, A.; Kale, K. S. *Inorg. Chem.* **1979**, *18*, 992–955.
(48) Colpas, G. J.; Hamstra, B. J.; Kampf, J. W.; Pecoraro, V. L. *J. Am. Chem. Soc.* **1996**, *118*, 3469–3478.
(49) Williams, D. H.; Fleming, I. *Spectroscopic Methods in Organic Chemistry*; Mc Graw-Hill: London, 1995.

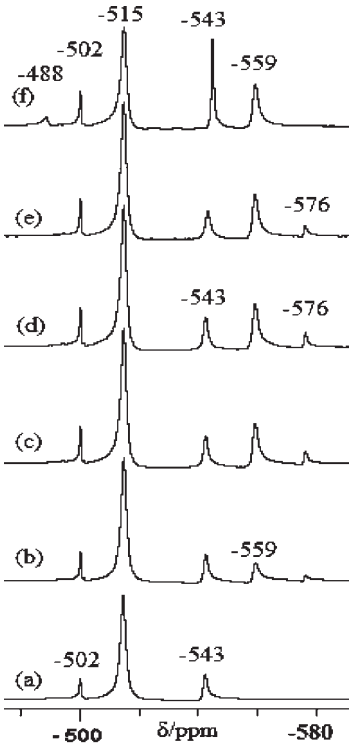

Figure 3. (a) ^{51}V NMR spectrum of a 4 mM solution of [$V^{V}O_2$(sal-dmen)] **4** in MeOH. The pH of this solution is ~8.0; (b) addition of 1.0 equiv of H_2O_2 (30%) to the solution of (a); (c) after addition of 2.0 equiv of H_2O_2 (total) (30%) to the solution of (a); (d) after addition of 5 equiv of H_2O_2 (30%) (total) to the solution of (a); the pH of this solution is ~4.0−4.5 (e) after addition of 0.5 equiv of HCl (11.6 M) to the solution of (d); (f) after addition of 1 equiv of HCl (total) to the solution of (e), the pH being ~3.5−4.0.

4 mM solution of **4** in DMSO shifts the −503 ppm resonances to −515 ppm, identical to the spectrum of **4** in MeOH only. This and other experiments carried out (see, e.g., Supporting Information) are consistent with assignment of the −503 ppm peak to **4** = **CI** (Scheme 4), and the −515 ppm resonance to [$V^{V}O_2$(sal-dmen)(MeOH)] (**4**·MeOH). The ^{51}V NMR resonance at −543 ppm probably corresponds to species [$V^{V}O_2$(sal-dmenH^{+})-(MeOH)] (**CII**·MeOH) which is formed from **CI** upon protonation, with the calculated ΔG_s value of −2.0 kcal/mol (Table 7). The calculated value for δ is −527 ppm. The tetra-coordinated complex **CII**, without the ligated methanol molecule (δ_{calc} = −438 ppm), and the octahedral complexes **CII**·2MeOH (δ_{calc} = −426 and −481 ppm, corresponding to two isomers) were found to be less stable than **CII**·MeOH by 5.5 and 13.5/22.8 kcal/mol, respectively (Table 7). The observed chemical shifts are within the values expected for dioxidovanadium(V) complexes containing a O/N donor set.[22] We emphasize that we could measure a good signal for the solid (powder) complex PS-[$V^{V}O_2$(fsal-dmen)] **2** suspended in DMSO, which presents a reasonably strong resonance at δ = −503/ −504 ppm (broad, line width at half height of ca. 300 Hz), see Figure 4.

A MeOH solution (ca. 4 mM) of complex **4** was divided in two portions. The addition of 1.0 equiv 30% aqueous solution of H_2O_2 to the first portion yielded a solution with pH about 4−4.5 and resonances at −559 and −576 ppm. These resonances could correspond to vanadate (V1) and divanadate (V2). However, if this was the case, for this solution and others discussed below where the pH is about 3−5 the resonances corresponding to decavana-

Scheme 4. Summary of Speciation of V-sal-dmen Species in Solution[a]

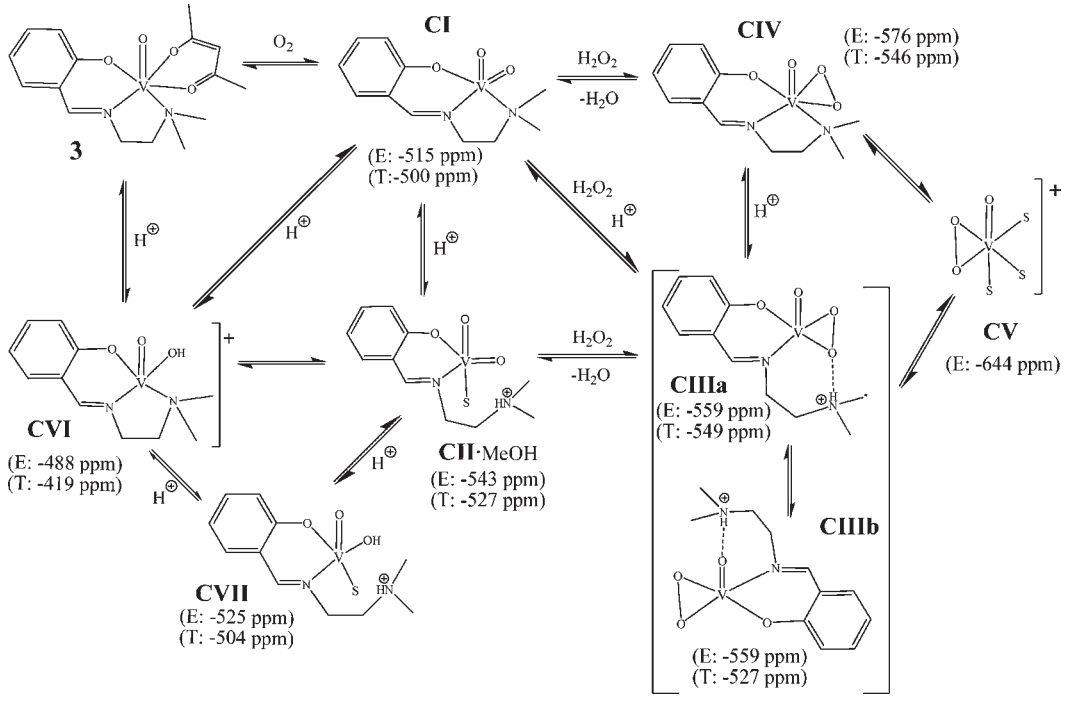

[a] The (E: xxx ppm) correspond to the measured ^{51}V NMR chemical shifts, and (T: yyy ppm) correspond to the DFT-calculated ^{51}V NMR chemical shifts for MeOH solutions (see text for details; the empirical correction of −42 ppm was added to the DFT chemical shifts of **CIII**, **CIV**, **CVIII**, and **CIX** calculated relative to $VOCl_3$, see also Computational Details for additional information). The acid added in the experiments was HCl; therefore, the counterion for the cationic complexes is Cl^{-} which may possibly closely associate to the complexes.

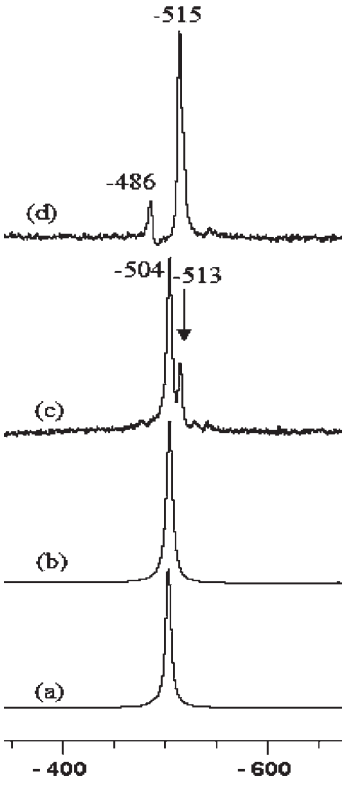

Figure 4. (a) ^{51}V NMR spectrum of suspension of PS-[$V^{V}O_2$(fsal-dmen)] **2** in DMSO; (b) solution of (a) after 24 h leaving tube open; (c) suspension of PS-[V^{IV}O(fsal-dmen)(MeO)] **1** in DMSO containing also an amount of acac estimated as 10 equiv after 24 h of contact with air; (d) addition of MeOH to the mixture of (c) so that the solvent is 1:1 of DMSO/MeOH.

date species would also appear in the ^{51}V NMR spectra, and this is not the case. Moreover, the signals observed are not pH-dependent. We assign the resonance at −559 ppm to [$V^{V}O(O_2)$(sal-dmenH$^+$)] (**CIII**), and the one at −576 ppm to [$V^{V}O(O_2)$(sal-dmen)] (**CIV**, see Scheme 4). Both these species may be formed from **CII**·MeOH and **CI**, respectively, with the calculated ΔG_s(MeOH) values of −5.3 and −1.3 kcal/mol, correspondingly (Table 7). On further additions of 30% aqueous solution of H_2O_2 to the solution (Figure 3b−d), the relative intensities of the −559 and −576 ppm peaks increase. Upon additions of a total of 0.5 and 1.0 equiv of an HCl solution (Figure 3e−f) a new peak at −488 ppm is detected, and the relative intensity of the resonance at −543 ppm increases (Figure 3f). We assign the resonance at −488 ppm to structure **CVI**, that is, to a oxidohydroxido-V(V) species, which is only by 1.7 kcal/mol less stable than **CII**·MeOH. The increase in the relative amount of **CII** is also compatible with the decrease of pH.

To the second portion of the MeOH solution (ca. 4 mM) of complex **4**, 1.0 + 1.0 equiv of an HCl solution (11.6 M) were added [see Supporting Information, Figure S3 (b) and (c)]. The new peak at −488 ppm is detected, the one at −543 ppm increased intensity, and the resonance at −515 ppm decreased intensity. This is in agreement with the assignments above (Scheme 4) involving the protonations of the ligand and of the oxido group. Upon further additions of the 30% aqueous solution of H_2O_2 a new

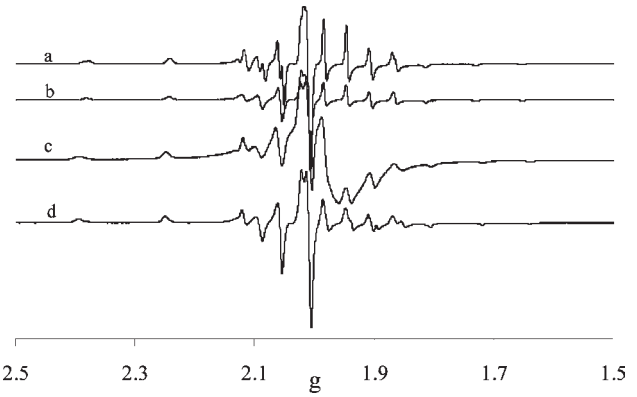

Figure 5. First derivative EPR spectra of frozen solutions of [V^{IV}O(sal-dmen)(acac)] (4 m M) (a) in MeOH; (b) in DMSO, (c) Solid sample of PS-[V^{IV}O(fsal-dmen)(MeO)] at room temperature, (d) Solid sample of PS-[V^{IV}O(fsal-dmen)(MeO)], suspended in DMSO, at 77 K.

resonance is detected at −559 ppm; it is assigned to **CIII** and results from protonation of the amine nitrogen of the *N*,*N*-dimethylethylenediamine ligand, thus forming [$V^{V}O(O_2)$(sal-dmenH$^+$)].[15d,e] As evaluated by DFT, both **CIIIa**- and **CIIIb**-type isomers may exist. However, only one species is detected by ^{51}V NMR assignable to the peroxo-protonated species. As the calculated ^{51}V NMR chemical shifts for **CIIIa** (−549 ppm, in MeOH) gives both a better absolute and relative agreement with the experimental one, we assign the −559 ppm resonance to **CIIIa**.

Upon further addition of H_2O_2 (viz. 3, 4, and 5 equiv), another resonance appears at −644 ppm which we tentatively assign as [$V^{V}O(O_2)(S)_n$] **CV** (S = solvent), shown in Scheme 4. Leaving the NMR tube open for 24 h at room temperature, the resonance at −515 ppm regains intensity, indicating the reversibility of the process.

A 4 mM solution of [V^{IV}O(sal-dmen)(acac)] **3** MeOH after 12 h of contact with air [Supporting Information, Figure S4 (a)] showed resonances at −515 and −544 ppm corresponding to the dioxido-complexes **CI** and **CII** (see Scheme 4). Upon stepwise additions of an aqueous solution of H_2O_2 [Supporting Information, Figure S4 (b−e)], the peaks at −559 ppm (1st), −576 ppm (2nd) (and −488 ppm) were detected, these results being compatible with the assignments given in Scheme 4. The presence of the acac ligand did not change neither the type of spectra obtained nor the chemical shifts recorded, indicating that the acac$^-$ ligand is not bound to the V(V)-complexes present in solution.

These experiments confirm that V^{V}-sal-dmen species are quite stable to additions of acid and/or H_2O_2 solutions, and only upon a relatively high excess of H_2O_2 (and acid) V^{V}-species not containing bound sal-dmen ligand are detected.

A suspension of PS-[$V^{V}O_2$(fsal-dmen)] **2** in DMSO gave a relatively strong resonance at about −503/−504 ppm, and a very small one at about −535 ppm, and the spectrum is exactly the same after 24 h (Figure 4a,b). This result is compatible with the presence of species **CI** in this polystyrene bound complex (PS-**CI**), the minor peak probably corresponding to PS-**CII**. In a distinct experiment a suspension of PS-[$V^{V}O_2$(fsal-dmen)] **2** in DMSO also containing an amount of acac estimated as 10 equiv,

Table 5. Spin Hamiltonian Parameters Obtained[21] from the Recorded Experimental EPR Spectra

compound	species	$g_{\|}$	$A_{\|} \times 10^4$ cm^{-1}	$A_{\perp} \times 10^4$ cm^{-1}	$g_{\perp}$
[V^{IV}O(sal-dmen)(acac)] **3**[a]	1st species	1.952	163.8	56.5	1.981
4 mM solution in MeOH	2nd species	1.953	161.7	55.9	1.981
[V^{IV}O(sal-dmen)(acac)] **3** 4 mM solution in DMSO		1.950	163.0	57.0	1.980
PS-[V^{IV}O(fsal-dmen)(MeO)] **1** Solid at room temperature		1.949	168.5	63.5	1.978
PS-[V^{IV}O(fsal-dmen)(MeO)] **1**[b]	1st species	1.947	168.5	55.7	1.978
suspended in DMSO for 12 h	2nd species	1.955	163.8	55.3	1.979
PS-[V^{IV}O(fsal-dmen)(MeO)] **1**	1st species	1.950	168.5	57.6	1.980
suspended in DMSO for 12 h, and freezing after about 3 min after addition of 10 equiv of Hacac	2nd species	1.952	163.5	55.4	1.981
PS-[V^{IV}O(fsal-dmen)(MeO)] **1** suspended in DMSO for 12 h, and freezing after about 3 h of addition of 10 equiv of Hacac		1.948	168.2	58.1	1.981
[V^{IV}O(sal-dmen)(acac)] **3**	1st species	1.952	169.5	57.2	1.981
spectrum of Figure 6c[c]	2nd species	1.952	163.8	55.9	1.980
	3rd species	1.953	161.2	56.9	1.979
[V^{IV}O(sal-dmen)(acac)] **3**	1st species	1.948	169.3	58.2	1.978
spectrum of Figure 6d[d]	2nd species	1.952	163.9	55.5	1.979
	3rd species	1.953	161.2	56.9	1.978

[a] The Spin Hamiltonian parameters of the two species are very close, and this does not allow accurate estimate of the spin Hamiltonian parameters. Probably they are isomeric species. [b] Spectrum recorded after swelling the solid in DMSO for 12 h. [c] After addition of 3.0 equiv of an H_2O_2 solution to a MeOH solution of **3** followed by 10 equiv of 2-methylthiophene. [d] Solution of Figure 6c after 2 h.

after 24 h of contact with air gave a similar spectrum with an additional peak at about −513 ppm (Figure 4c). Addition of methanol to this solution gave a ^{51}V NMR spectrum (Figure 4d) compatible with the formation of a species corresponding to **CI**·MeOH and **CVI** (Scheme 4).

In another experiment stepwise additions of aqueous solution of H_2O_2 were made to a suspension of PS-[$V^{V}O_2$(fsal-dmen)] **2** in DMSO. Upon addition of 2 equiv of H_2O_2 (the mixture becomes slightly more acidic) the peak at about −535 ppm increases its intensity, while a very minor one is detected at about −576 ppm, probably corresponding to PS-[$V^{V}O(O)_2$(fsal-dmen)] suspended in DMSO, that is, it is probably the polymer-bound version of **CIV**.

EPR Spectroscopy Study. The EPR spectra of "frozen" (77 K) solutions (in MeOH and DMSO) of [V^{IV}O(sal-dmen)(acac)] **3** were recorded, as well as that of solid PS-[V^{IV}O(fsal-dmen)(MeO)] **1** (at room temperature and 77 K). The spectra are depicted in Figure 5.

The spin Hamiltonian parameters obtained by simulation[21] of the experimental EPR spectra are included in Table 5. For complex **3** dissolved in MeOH, two species with quite similar $A_{||}$ values (of 163.8 and 161.7 × 10^{-4} cm^{-1}) were obtained, while in DMSO only one component with $A_{||} = 163 \times 10^{-4}$ cm^{-1} was detected. Once a particular binding mode is assumed, the values of $A_{\|}$ can be estimated using the additivity relationship proposed by Wurthrich[50] and Chasteen,[51] with estimated accuracy of $\pm 3 \times 10^{-4}$ cm^{-1}. However, for the donor groups under consideration their predicted contributions to the parallel hyperfine coupling constant are rather similar (O_{acac} ~41.7; $O_{phenolate}$ ~38.9; N_{imine} ~41.6; N_{amine} ~40.1, O_{DMSO} ~41.9; O_{MeOH} ~45.5, all $A_{||}$ contributions in cm^{-1} × 10^4),[50−52] so it is not possible to distinguish between the several plausible binding modes. However, the hyperfine features and spectra of [V^{IV}O(sal-dmen)-(acac)] **3** are consistent with binding modes involving either $(O_{acac}, O_{phenolate}, N_{imine}, N_{amine})_{equatorial}(O_{acac})_{axial}$ or $(2 \times O_{acac}, O_{phenolate}, N_{imine},)_{equatorial}(N_{amine})_{axial}$. Only one species is found in DMSO solution, and the spin Hamiltonian parameters are similar to those in MeOH, this ruling out participation of solvent molecules in the coordination sphere. Therefore the two complexes detected in MeOH solution probably correspond to isomeric species.

The resolved EPR pattern of spectrum of solid **1** indicates that the $V^{IV}O$-centers are reasonably well dispersed in the polymer matrix, but some dipolar interactions exist. Neverthesess, the spin Hamiltonian parameters could be obtained and are in good agreement with a O_2N_2 binding mode. Solid **1** shows only one species at room temperature with $A_{||}$ (168.5×10^{-4} cm^{-1}) and, comparing with the spectra obtained for **3**, does not indicate the presence of acac$^-$ as secondary ligand. In fact the $A_{||}$ value indicates participation of solvent (MeOH) in the equatorial position. The EPR spectrum of solid **1** suspended in DMSO for 12 h shows the presence of a minor species with lower value of $A_{||}$ (163.8×10^{-4} cm^{-1}). This could either correspond to the involvement of the DMSO at the equatorial position, instead of MeOH, or to the presence of a small amount (ca. 5%) of PS-[V^{IV}O(fsal-dmen)(acac)]. However, addition of 10 equiv of Hacac to this solid suspended in DMSO does not change much the $A_{||}$ value (163.5 × 10^{-4} cm^{-1}); therefore, we find no indication for the binding of an acac$^-$ ligand in solid **1**. The ^{51}V NMR of this solution suspended in DMSO for 36 h (Figure 4) in the presence of air shows resonances at −504 and −513 ppm, similar to the samples of PS-[$V^{V}O_2$(fsal-dmen)] **2** suspended in DMSO. Scheme 5 summarizes these results.

(50) Wurthrich, K. *Helv. Chim. Acta* **1965**, *48*, 1012–1017.
(51) Chasteen, N. D. In *Biological Magnetic Resonance*; Reuben, J. Ed.; Plenum: New York, 1981; p 53.
(52) (a) Butenko, N.; Tomaz, I.; Nouri, O.; Escribano, E.; Moreno, V.; Gama, S.; Ribeiro, V.; Telo, J. P.; Costa Pesssoa, J.; Cavaco, I. *J. Inorg. Biochem.* **2009**, *103*, 622–632. (b) Garribba, E.; Micera, G.; Sanna, D. *Inorg. Chim. Acta* **2006**, *359*, 4470–4476. (c) Rehder, D.; Weidemann, C.; Duch, A.; Priebsch, W. *Inorg. Chem.* **1988**, *27*, 584–587. (d) Correia, I.; Costa Pessoa, J.; Duarte, M. T.; Henriques, R. T.; Piedade, M. F. M.; Veiros, L. F.; Jackush, T.; Dornyei, A.; Kiss, T.; Castro, M. M. C. A.; Geraldes, C. F. G. C.; Avecilla, F. *Chem.—Eur. J.* **2004**, *10*, 2301–2317. (e) Butler, A.; Clague, M. J.; Meister, G. E. *Chem. Rev.* **1994**, *94*, 625–638.

Scheme 5. Formation of Complex **2** Either Directly from **1** or Also through the Addition of $[V^{IV}O(acac)_2]$ to the PS-Anchored Ligand **I**, Followed by Air Oxidation

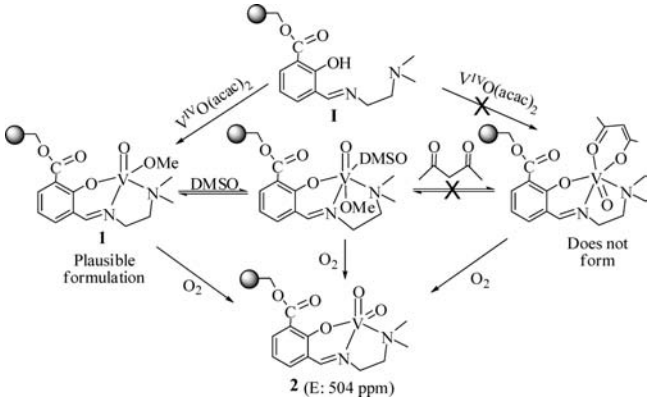

Scheme 6. Conversion of Organosulfur Compounds to the Corresponding Sulfones Catalyzed by the Vanadium Complexes

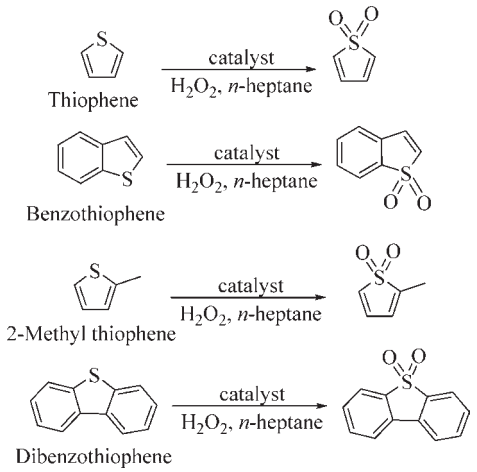

Catalytic Activity. Catalytic Desulfurization of Organosulfur Compounds. The catalytic potential of polymer-bound complex, PS-$[V^{V}O_2$(fsal-dmen)] **2** was checked for the selective oxidation of different organosulfur compounds such as T, BT, 2-methylthiophene (MT), and DBT with the concentration of 500 ppm sulfur. All substrates were converted to the corresponding sulfones; Scheme 6. The products were identified by gas chromatography and further confirmed by GC-MS. Various parameters: temperature of the reaction mixture, amount of catalyst, and oxidant were optimized considering thiophene (T) as a representative substrate.

The oxidation of the organosulfur compounds depends on the amount of oxidant, H_2O_2, used for the reaction. Reactions were carried out at three different oxidant to substrate ratios of 2:1, 3:1, and 4:1 using thiophene (S concentration 500 ppm) and catalyst (0.0715 mmol) at 60 °C. As illustrated in the Supporting Information, Figure S7 , a maximum of 83.3% desulfurization has been achieved within 2 h of reaction time at a H_2O_2 to S molar ratio of 2:1. Increasing this ratio to 3:1 led to a desulfurization of about 99.8%, while 4:1 molar ratio obviously showed no further improvement in desulfurization. In another set of experiments, three different catalyst loadings, namely, 0.0356 mmol, 0.0715 and 0.1075 mmol were considered at a S to H_2O_2 ratio of 1:3 under the above reaction conditions, and the results are presented in Supporting Information, Figure S8. As seen in the figure, 0.0356 mmol of catalyst gave only 82% desulfurization while 0.0715 and 0.1075 mmol of catalyst loadings have shown a comparable desulfurization of 99.8 and 99.7%, respectively. Thus, 0.0715 mmol of catalyst is considered to be adequate to carry out the reaction for maximum oxidation. The temperature of the reaction mixture has also significant influence on the performance of the catalyst. As shown in Supporting Information, Figure S9, running the reaction at 60 °C gave a much better yield of the reaction products (close to 100% after 90 min.), than at room temperature, while reaction at 80 °C gave only faster achievement of about 100% conversion.

Thus, the optimized reaction conditions established for the maximum desulfurization of thiophene (500 ppm of S) in *n*-heptane are 1 : 3 S to H_2O_2 molar ratio, catalyst precursor PS-$[V^{V}O_2$(fsal-dmen)] **2** (0.0715 mmol), and temperature (60 °C). Under these optimized reaction conditions we have also tested the catalytic activity of the polymer-bound complex PS-$[V^{IV}O$(fsal-dmen)(MeO)] **1** and of complexes **3** and **4**, and the progress of the desulfurization of organosulfur compounds as a function of time is presented in Table 6. Complexes **3** and **4** are not soluble in *n*-heptane and can be separated by filtration after the reaction. In conditions similar to those of the reactions presented in Table 6, but in the absence of catalysts, the conversions were thiophene (9.0%), benzothiophene (6.5%), dibenzothiophene (5.2%), and 2-Methylthiophene (8.4%).

Mechanism of Desulfurization of Model Diesel Mixtures. Our catalytic systems is based on either oxidovanadium(IV) or dioxidovanadium(V) complexes. We have used 2-methylthiophene as a model substrate to investigate the intermediate species formed during the desulfurization of model diesel mixtures.

To find evidence for the intermediate species formed during the catalytic cycle we studied the interaction of $[V^{IV}O$(sal-dmen)(acac)] **3** with 2-methylthiophene by EPR. Different amounts of H_2O_2 were added to the neat complex $[V^{IV}O$(sal-dmen)(acac)] **3** dissolved in MeOH (4 mM) (see Figure 6). After addition of about 3 equiv of H_2O_2, a very weak EPR signal was obtained, indicating the oxidation of the metal center (Figure 6b). Addition of 2-methylthiophene to this solution resulted in reduction of the metal center to oxidovanadium(IV) species (see Figure 6c,d). Globally three distinct species could be detected, the spin Hamiltonian parameters obtained being included in Table 5. The complexes formed correspond to $[V^{IV}O$(sal-dmen)(acac)] **3** and $[V^{IV}O$(sal-dmen)-$(S)_n]$ (S = MeOH/H_2O), that is, addition of H_2O_2 solution, followed by 2-methylthiophene completes an oxidation/reduction cycle where **3** may not be preserved, but $[V^{IV}O$-(sal-dmen)$(S)_n]$ regains its integrity.

Solutions of $[V^{IV}O$(sal-dmen)(acac)] **3** in methanol are sensitive toward addition of H_2O_2, as monitored by electronic absorption spectroscopy, yielding oxidoperoxo species. Figure 7a presents the spectral changes observed for **3**. Thus, the progressive addition of a dilute H_2O_2 solution in methanol to a solution of $[V^{IV}O$(sal-dmen)-(acac)] **3** in methanol results in flattening/disappearance of bands appearing at 813 (d-d band) and 538 nm (partly a

Table 6. Desulfurization of Model Diesel Mixture[a]

catalyst	sulfur containing compounds	sulfur content (in ppm) initial concentration	sulfur content (in ppm) after desulfurization	sulfur removal (%)
1	thiophene	500	65.5	86.9
1[b]		500	66.9	86.6
1[c]		500	66.8	86.6
1	benzothiophene	500	63	87.4
1[b]		500	64.8	87
1[c]		500	65.1	87
1	dibenzothiophene	500	60.5	87.9
1[b]		500	62.1	88.6
1[c]		500	61.8	87.6
1	2-methylthiophene	500	57.5	88.5
1[b]		500	57.9	88.4
1[c]		500	58.7	88.2
2	thiophene	500	9.5	98.1
2[b]		500	9.4	98.1
2[c]		500	10.1	97.9
2	benzothiophene	500	8.5	98.3
2[b]		500	9	98.2
2[c]		500	9.9	98
2	dibenzothiophene	500	8	98.4
2[b]		500	8.7	97.6
2[c]		500	8.5	97.7
2	2-methylthiophene	500	6	98.8
2[b]		500	6.7	98.7
2[c]		500	7.1	98.6
3	thiophene	500	148.5	70.3
3[b]		500	149.7	70.1
3[c]		500	149.6	70.1
3	benzothiophene	500	144.5	71.1
3[b]		500	145.9	70.8
3[c]		500	146.5	70.7
3	dibenzothiophene	500	141.5	71.7
3[b]		500	141.9	71.6
3[c]		500	140.8	71.8
3	2-methylthiophene	500	140.5	71.9
3[b]		500	142.7	71.5
3[c]		500	141.6	71.7
4	thiophene	500	113	77.4
4[b]		500	113.8	77.2
4[c]		500	113.6	77.3
4	benzothiophene	500	109.5	78.1
4[b]		500	110.7	77.8
4[c]		500	110.5	77.9
4	dibenzothiophene	500	111.5	77.7
4[b]		500	112.8	77.4
4[c]		500	113.5	77.3
4	2-methylthiophene	500	108	78.4
4[b]		500	108.5	78.3
4[c]		500	108.3	78.3

[a] Percentage and reaction products using anchored oxido- and dioxido-vanadium catalysts.[d] Reaction conditions: organosulfur compound (equivalent to 500 ppm of S) in *n*-heptane, H_2O_2 (3 × molar excess of the corresponding organosulfur compound), that is, oxidant: substrate ratio of 3:1, catalyst (0.0715 mmol), temperature (60 °C), and time = 2h. [b] 2nd catalytic cycle data. [c] 3rd catalytic cycle data. [d] To avoid contaminations of metal ion in GC column the contents were first extracted with acetonitrile before injections.

d-d band). The intensity of the 322 and 239 nm bands slowly decrease and disappear, while the intensity of the 259 and 215 nm bands increases. These changes indicate the oxidation of the metal center and formation of peroxo-complexes.

As mentioned above, we prepared complex [$V^{V}O(O_2)$(sal-dmen)]; however, as it is unstable and loses oxygen at room temperature it could not be properly characterized. Peroxo-to-vanadium charge transfer transitions have been reported at λ_{max} ~450 nm.[48,53] The electronic spectrum of this complex exhibits a rather strong broad band at about 390 nm, the broadness of this band suggesting interference of the peroxo-to-vanadium charge transfer transition with band involving the C=N group.

The UV−vis spectral changes during a similar titration of **4** with H_2O_2 (diluted in methanol) is shown in Figure 7b. With low amounts of H_2O_2 added no appreciable changes in band positions were observed, but further additions of H_2O_2 yielded a final spectrum which is very similar to that obtained in the titration of [$V^{IV}O$(sal-dmen)(acac)] **3**

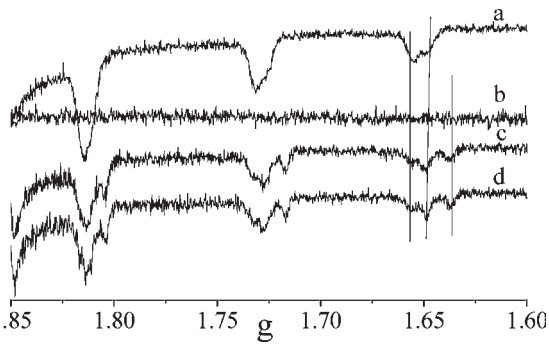

Figure 6. High field region of the first derivative EPR spectra of frozen (77 K) solutions of [$V^{IV}O$(sal-dmen)(acac)] (4 mM) (a) in MeOH; (b) addition of 3 equiv of H_2O_2 to the solution of (a); (c) addition of 10 equiv of 2-methylthiophene to the solution of (b); (d) solution of (c) after 2 h.

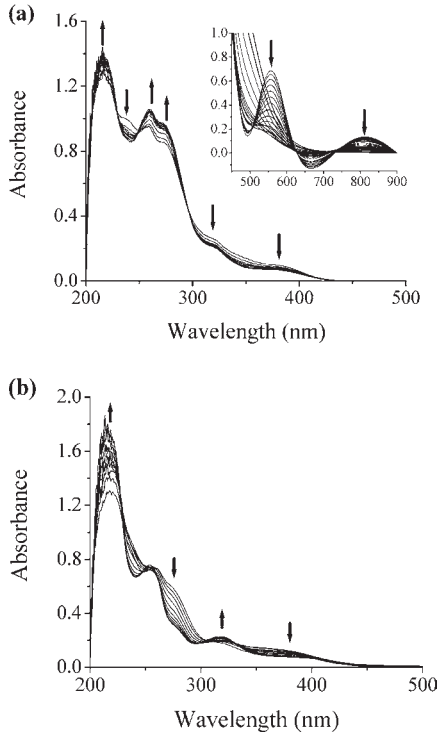

Figure 7. UV−vis spectral changes observed during titration of (a) [$V^{IV}O$(sal-dmen)(acac)] **3** and of (b) [$V^{V}O_2$(sal-dmen)] **4** with H_2O_2. The spectra were recorded after stepwise additions of one drop portions of H_2O_2 (6.6×10^{-4} mmol of 30% H_2O_2 dissolved in 10 mL of methanol) to 50 mL of about 10^{-4} M solution of either (a) **3**, or (b) **4** in methanol; the inset shows equivalent titration with ca. 10^{-3} M solution.

(53) Hamstra, B. J.; Colpas, G. J.; Pecoraro, V. L. *Inorg. Chem.* **1998**, *37*, 949–955.

Table 7. DFT-Calculated Reaction Energies (kcal/mol) for Gas-Phase, MeOH Solution [in Parentheses], and *n*-heptane Solution [in {} Brackets]

reaction	ΔE	ΔH	ΔG
CI + H_2O_2 → **CIV** + H_2O	−4.2 (−1.3)	−4.8 (−2.0)	−3.9 (−1.3)
CI + H_3O^+ + MeOH → **CII·MeOH** + H_2O	−86.2 (−10.7)	−84.1 (−8.6)	−73.5 (−2.0)
CI + H_3O^+ → **CVI** + H_2O	−61.0 (0.5)	−61.9 (−0.4)	−61.8 (−0.3)
CVI → **CII**	2.4 (2.7)	3.8 (4.1)	3.4 (3.8)
CII + MeOH → **CII·MeOH**	−27.6 (−13.8)	−26.0 (−12.2)	−15.1 (−5.5)
CII·MeOH + H_3O^+ → **CVII** + H_2O	18.5 (11.2)	17.5 (10.1)	16.9 (9.7)
CII·MeOH + MeOH → **CII·2MeOH**[a]	−8.3 (5.2)	−7.0 (6.6)	4.3 (13.5)
	1.0 (15.1)	1.8 (15.9)	12.9 (22.8)
CI + H_2O_2 + H_3O^+ → **CIIIa** + 2 H_2O	−71.3 (−6.9)	−71.6 (−7.1)	−69.8 (−5.9)
	{−50.4}	{−50.6}	{−49.1}
CI + H_2O_2 + H_3O^+ → **CIIIb** + 2 H_2O	−75.3 (−8.5)	−75.3 (−8.5)	−73.5 (−7.3)
	{−53.8}	{−53.8}	{−52.2}
CII·MeOH + H_2O_2 → **CIIIb** + H_2O + MeOH	11.9 (2.1)	8.8 (0.1)	0.0 (−5.3)
CIV + H_3O^+ → **CIIIb** + H_2O	−71.1 (−7.2)	−70.5 (−6.5)	−69.6 (−6.0)
CIIIb → **CIIIa**	4.0 (1.6)	3.7 (1.4)	3.7 (1.4)
	{3.4}	{3.2}	{3.1}
CIIIb + MeOH → **CIIIb·MeOH**	−11.9 (1.2)	−10.4 (2.8)	1.1 (9.9)
CIIIa → **CVIII**	2.6 (4.1)	2.3 (3.8)	3.1 (4.3)
	{1.9}	{1.5}	{2.2}
CIIIb → **CVIII**	6.6 (5.8)	6.0 (5.2)	6.8 (5.7)
	{5.2}	{4.6}	{5.3}
CIIIb → **CIX**	11.6 (12.4)	9.8 (10.7)	10.8 (11.4)
	{10.4}	{8.6}	{9.5}
CIX → **CVIII**	−5.0 (−6.7)	−3.8 (−5.5)	−4.1 (−5.7)

[a] Two isomers were found for the formulation of **CII·2MeOH**.

with H_2O_2, thus demonstrating that the same oxidoperoxovanadium(V) species form upon addition of H_2O_2 to methanolic solutions of either **3** or **4**.

The ^{51}V NMR spectrum of [V^VO_2(sal-dmen)] **4** dissolved in MeOH showed resonances at −515 (∼91%), minor −502 (∼3%) and −544 ppm (∼6%) (see Figure 8a). Upon the stepwise addition of an aqueous 30% solution of H_2O_2 to this solution the peak at −515 ppm progressively decreases intensity while resonances at −559 ppm and −576 ppm are observed, corresponding to **CIII** and **CIV** (see Figure 8b−d, and assignments in Scheme 4). Upon further stepwise additions of H_2O_2 (5 equiv or higher) a new signal at δ = −644 ppm is detected, which we assign to inorganic monoperoxo-vanadates.[54] Upon addition of 2-methylthiophene, the sulphoxidation process occurs slowly at room temperature, the peroxo-V^V-complexes are consumed, and the V^VO_2-complexes corresponding to **CI** (and **CII**) form, indicating the reversibility of the process. Taking into account the results described above when discussing Figure 6, $V^{IV}O$-species also form upon addition of 2-methylthiophene, but it was possible to record good quality ^{51}V NMR spectra. The final ^{51}V NMR spectrum was almost identical to the initial spectrum of **4**, showing that the dioxidovanadium(V) catalyst precursor is retained after completion of the reaction.

Inorganic vanadium(V) peroxo-compounds have been reported to mediate several types of oxygen-transfer reactions, namely, the oxidation of a variety of organic sulfides to sulfoxides and sulfones in the presence of hydrogen peroxide or *tert*-butyl hydroperoxide catalyzed by V^V-species in organic solvents.[15e,55] The sulfur atom of 2-methylthiophene is electron rich and undergoes electrophilic oxidation yielding the corresponding sulfoxide and

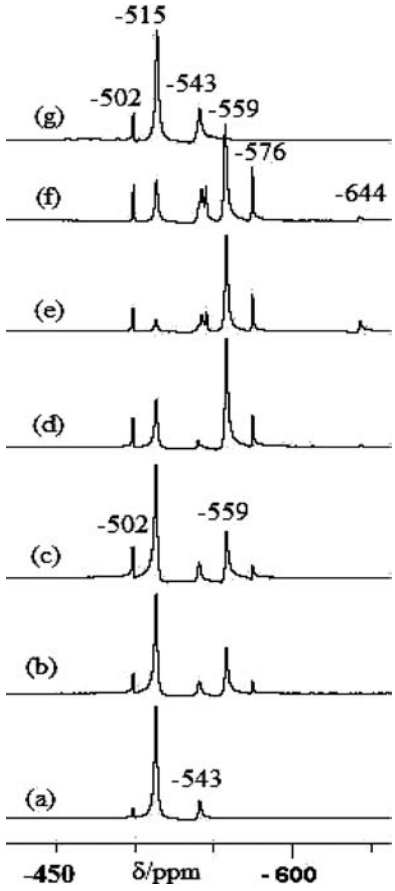

Figure 8. (a) ^{51}V NMR spectrum of a 4 mM solution of [V^VO_2(sal-dmen)] **4** in MeOH; (b) addition of 1.0 equiv of H_2O_2 (30%) to the solution of (a); (c) after addition of a total of 2.0 equiv of H_2O_2 (30%) to the solution of (a); (d) after addition of a total of 5 equiv of H_2O_2 (30%) to the solution of (a); (e) after addition of a total of 6.0 equiv of H_2O_2 (30%) to the solution of (a); (f) after addition of 10 equiv of 2-methylthiophene to the solution of (e); (g) 36 h after recording spectrum (f).

(54) Pettersson, L.; Andersson, I.; Gorzás, A. *Coord. Chem. Rev.* **2003**, *237*, 77–87.
(55) Bortolini, O.; Di Furia, F.; Modena, G. *J. Mol. Catal.* **1982**, *16*, 61–68.

Scheme 7. Relevant Species Involved in the Evaluation of the Energetics of Formation of **CVIII**, Considered the Active Catalytic Species[a]

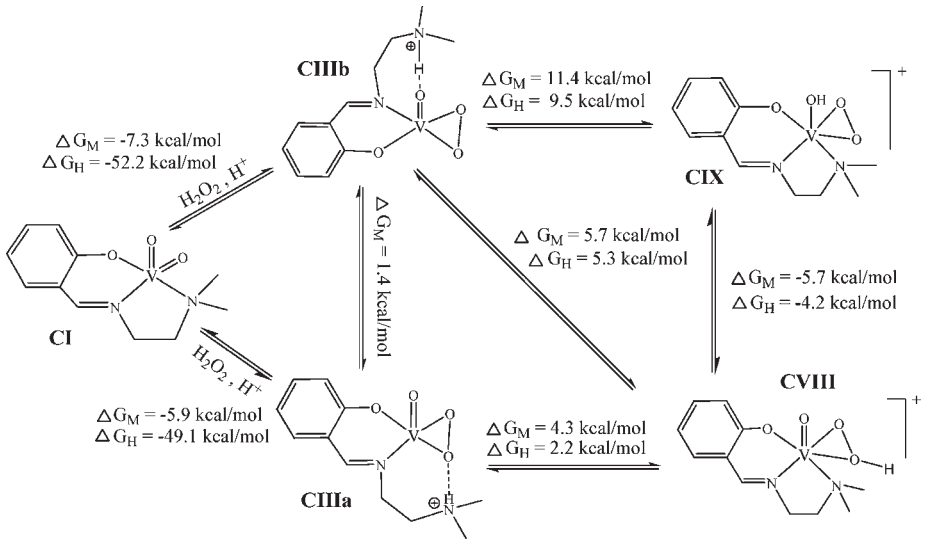

[a] The values of ΔG included were calculated by DFT (B3P86), ΔG_M for methanol, and ΔG_H for heptane as solvent. The large difference of ΔG values of the conversions of **CIb** to **CIIIa**, **CIIIb** between methanol and heptane is due to the lower stabilization of H_3O^+ in heptane.

Scheme 8. General Outline of Reaction Mechanism of Oxidation of Thioethers with $[V^{IV}O(sal\text{-}dmen)(acac)]$ **3** or $[V^{V}O_2(sal\text{-}dmen)]$ **4** As Catalyst Precursors[a]

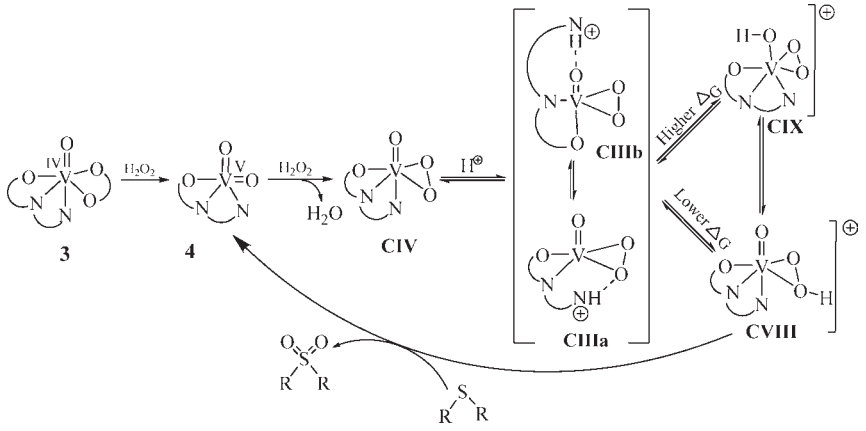

[a] The pathway through $[V^{V}(OH)(O_2)(sal\text{-}dmen)]^+$ (**CIX**) is not expected to occur.

sulfone. Similar reactions may proceed with the other sulfides (thiophene, dibenzothiophene, and benzothiophene) tested in this work. The ^{51}V NMR spectra recorded indicate clearly that complex **4**, on treatment with H_2O_2, is able to generate peroxo-vanadium(V) complexes including protonated peroxo V^V-complexes, the formation of species **CIIIa**, a complex with a structure resembling that of the hydroperoxovanadium(V) complex **CVIII**, being plausible. The formation of the hydroperoxo ligand, enhances the electrophilicity of the peroxo ligand, and **CVIII** is expected to be the active catalytic intermediate. It may react easily with the sulfides studied here, thereby explaining the desulphurization of the model fuel diesel tested. The proposed catalytic cycle for oxidation of 2-methylthiophene as model reaction is given in Scheme 8[56−59]

DFT calculations were carried out, and the gas-phase structures, the MeOH (and heptane in some cases) solution structures, and the corresponding ^{51}V NMR chemical shifts were calculated for all species included in Scheme 4. In the Supporting Information we include tables with total energies, enthalpies, Gibbs free energies, and entropies of the calculated structures, as well as some figures and schemes. Scheme 7 summarizes data for some of the relevant species formed.

For all complexes depicted in Schemes 4 and 7, except **3**, the DFT calculations of the equilibrium structures were carried out. The calculations indicate that the formation of **CVIII** from **CIIIa** is moderately endoergonic (ΔG_s(MeOH) = +4.3 kcal/mol) while the reaction

(56) Adão, P.; Costa Pessoa, J.; Henriques, R. T.; Kuznetsov, M. L.; Avecilla, F.; Maurya, M. R.; Kumar, U.; Correia, I. *Inorg. Chem.* **2009**, *48*, 3542–3561.
(57) Kuznetsov, M. L.; Costa Pessoa, J. *Dalton Trans.* **2009**, 5460–5468.
(58) Schneider, C. J.; Penner-Hahn, J. E.; Pecoraro, V. L. *J. Am. Chem. Soc.* **2008**, *130*, 2712–2713.
(59) Rehder, D. *Bioinorganic Vanadium Chemistry*; John Wiley & Sons: New York, 2008; p 115.

CIIIa → **CIX** requires significantly higher energy (ΔG_s(MeOH) = +10.0 kcal/mol). These findings agree with those of Schneider et al.[58] for the [$V^VO(O_2)$Hheida] system (H_3heida = *N*-(2-hydroxyethyl)iminodiacetic acid), these authors reporting spectroscopic evidence that protonation of the oxido-moiety does not occur under catalytic conditions (e.g., in sulfoxidations).

Table 7 summarizes calculated relevant data for several reactions in gas-phase, MeOH (M), and *n*-heptane (H) solution. As indicated in Table 7 the formation of the hydroperoxo complex **CVIII**, expected to be the active catalytic species for oxygen transfer by the direct attack of the substrate to the nonprotonated peroxo oxygen, is less endoergonic than **CIX**.[59]

We believe that the good efficiency of the present V-sal-dmen system may be related to the formation of species **CIIIa** (or **CIIIb**) and their good stability (see, e.g., Figures 3 and 8), and the relatively low ΔG values involved in the formation of the hydro-peroxo species **CVIII** [as far as can be inferred from the ΔG_S(MeOH) of the processes **CIIIb** → **CVIII** or **CIIIa** → **CVIII**]. As expected in heptane the ΔG values involved in the formation of **CIII** are significantly higher.

With the polystyrene anchored complexes **1** and **2** the mechanism of the sulfoxidation is expected to be similar to that operating with **3** or **4**. The efficiency of sulfur removal was clearly higher with **1** and **2** than with the neat complexes **3** and **4**, probably partly because the integrity of the catalysts is better preserved in the anchored complexes, and partly because all organosulfur compounds tested are aromatic-type compounds, expected to have good affinity for the polystyrene matrix. Additionally, Table 6 shows that all systems do not loose efficiency for sulfoxidations with *n*-heptane as solvent, at least up to the third cycle of reaction, this indicating that all preserve their integrity under the conditions used.

Scheme 8 gives a global outline of the reaction mechanism of oxidation of thioethers with [V^{IV}O(sal-dmen)(acac)] **3** or [V^VO_2(sal-dmen)] **4** as catalyst precursors.

Conclusions

The polymer-bound ligand, PS-Hfsal-dmen (**I**), with the fsal-dmen covalently bonded to polystyrene cross-linked with 5% divinylbenzene, was prepared. Upon treatment of **I** with [$V^{IV}O(acac)_2$] in the presence of MeOH the complex PS-[V^{IV}O(fsal-dmen)(MeO)] **1** was obtained. The V^{IV}-complex **1** in methanol was oxidized by air to PS-[V^VO_2(fsal-dmen)] **2**. The neat complexes, [V^{IV}O(sal-dmen)(acac)] **3** and [V^VO_2(sal-dmen)] **4**, were also prepared, and their molecular structures were determined by single crystal X-ray diffraction.

The EPR spectrum of the polymer supported V^{IV}O-complex **1** is characteristic of a magnetically diluted V^{IV}O-complex with a N,O binding set. Good ^{51}V NMR spectra could also be measured with PS-[V^VO_2(fsal-dmen)] **2** suspended in DMSO, and the chemical shift obtained (−503 ppm) is compatible with a $V^VO_2^+$-center and a N,O binding set. ^{51}V NMR experiments with [V^VO_2(sal-dmen)] **4** confirm that V^V-sal-dmen species are quite stable to additions of acid and/or H_2O_2 solutions, and only upon a relatively high excess of H_2O_2 (and acid) V^V-species not containing bound sal-dmen ligand are detected. With the help of DFT all V^V-species detected by ^{51}V NMR were assigned, and the speciation for the system is summarized in Scheme 4.

The catalytic oxidative desulfurization of model fuel diesel mixtures of organosulfur compounds such as thiophene, dibenzothiophene, benzothiophene, and 2-methyl thiophene were carried out in *n*-heptane using complexes **1**−**4**. The thioeher-sulfur in model organosulfur compounds was efficiently oxidized to the corresponding sulfone in the presence of H_2O_2. The systems **1**−**4** do not loose efficiency for sulfoxidations at least up to the third cycle of reaction, this indicating that all are recyclable under the conditions used.

Plausible intermediates involved in these catalytic processes were established by UV−vis, EPR, ^{51}V NMR, and DFT studies; namely, complex **4** in methanol, on treatment with H_2O_2, is able to generate peroxo-vanadium(V) complexes including quite stable protonated peroxo-V^V-complexes formulated as [$V^VO(O)_2$(sal-dmen-NH^+)]. An outline of the mechanism is proposed involving an hydro-peroxovanadium(V)-sal-dmen complex as the active catalytic species. The data indicate that formation of the intermediate hydroxido-peroxo-V^V complex [V^V(OH)(O_2)(sal-dmen)]$^+$ does not occur, but instead protonated [$V^VO(O)_2$(sal-dmen-NH^+)] complexes are relevant for catalytic action.

Acknowledgment. M.R.M. and A.A. are thankful to Council of Scientific and Industrial Research for financial support. J.C.P. and A.K. thank the Portuguese NMR Network (IST-UTL Center), and the POCI 2010, FEDER, Fundação para a Ciência e Tecnologia, SFRH/BPD/34835/2007, PTDC/QUI-QUI/098811/2008 and PTDC/QUI-QUI/112015/2009 for financial support. M.L.K. is grateful to the FCT and IST for a research contract within Ciência 2007 scientific programme.

Supporting Information Available: Description of molecular structures determined by single-crystal X-ray diffraction, FE-SEM and EDX studies, additional ^{51}V NMR experiments, optimization of catalytic reactions, IR and UV−vis absorption spectra of [$VO(O_2)$(sal-dmen)] and DFT computational details (tables with structural parameters of CI, absolute and relative energies, chemical shifts, Cartesian atomic coordinates for equilibrium structures). This material is available free of charge via the Internet at http://pubs.acs.org.